# Three-Phase Flash in Compositional Simulation Using a Reduced Method

**R. Okuno,*** **R.T. Johns,** and **K. Sepehrnoori,** SPE, The University of Texas at Austin

## Summary

$CO_2$ flooding at low temperatures often results in three or more hydrocarbon phases. Multiphase compositional simulation must simulate such gasfloods accurately. Drawbacks of modeling three hydrocarbon phases are the increased computational time and convergence problems associated with flash calculations. Use of a reduced method is a potential solution to these problems.

We first demonstrate the importance of using three-phase flash calculations in compositional simulation by investigating difficulties with two-phase equilibrium approximations proposed in the literature. We then extend an algorithm for reduced two-phase flash calculations to three-phase calculations and show the efficiency and robustness of our algorithm. The reduced three-phase flash algorithm is implemented in a multiphase compositional simulator to demonstrate the speed-up and increased robustness of simulations in various case studies.

Results show that use of a two-phase equilibrium approximation in reservoir simulation can result in a complete failure or erroneous simulation results. Simulation case studies show that our reduced method can decrease computational time significantly without loss of accuracy. Computational time is reduced using our reduced method because of the smaller number of equations to be solved and increased timestep sizes. We show that a failure of a flash calculation leads directly to reduced timestep sizes using the UTCOMP simulator.

## Introduction

Mixtures of reservoir oil and solvent such as $CO_2$ and rich gas can exhibit complex phase behavior at low temperatures where a third solvent-rich liquid phase can coexist with the oleic and gaseous phases (Shelton and Yarborough 1977; Orr et al. 1981; Henry and Metcalfe 1983; Turek et al. 1988; Creek and Sheffield 1993). Reliable numerical simulation of gasfloods involving such complex phase behavior requires robust phase-equilibrium algorithms capable of handling at least three hydrocarbon phases. However, most compositional simulators do not attempt to solve for three hydrocarbon phases because three-phase-equilibrium calculations are more complicated, difficult, and time-consuming than traditional two-phase-equilibrium calculations.

Nghiem and Li (1986) studied the importance of a third hydrocarbon phase in multiphase compositional simulation by comparing simulation results with two-phase-equilibrium calculations to those with three-phase-equilibrium calculations. In their simulations with only two-phase-equilibrium calculations, two-phase calculations are performed even in the three-phase region. They concluded that the two-phase-equilibrium approximation can be used with little loss of accuracy because the three-phase region exists only over a small part of the reservoir. However, their conclusion was based on 1D slimtube simulations using only two recombined oils from the same field. Several authors later demonstrated that the proper use of three-phase-equilibrium calculations gives simulation results that are significantly different from those with two-phase-equilibrium calculations (Khan et al. 1992; Wang and Strycker 2000; Guler et al. 2001). Also, as reported by Khan (1992) and Wang and Strycker (2000), convergence problems can occur when attempting to approximate such low-temperature gasfloods using only two-phase-equilibrium calculations, and, in some cases, the simulations cannot be completed. In this paper, we explain one reason for potential convergence problems associated with the two-phase-equilibrium approximation.

To overcome the drawbacks of simulation involving three hydrocarbon phases, Fong et al. (1992) proposed another way to approximate three-hydrocarbon-phase simulations. They characterized fluids that exhibit three-phase equilibrium in such a way that the resulting equation-of-state (EOS) model predicts no three-phase region. They reported that simulation results with the two-phase-equilibrium approximation agree well with the field data when the minimum miscibility pressure (MMP) simulated with the two-phase representation matches the experimentally determined MMP. However, as will be discussed in this paper, the approximation procedure requires significant tuning of EOS parameters. Because their approximation procedure has no theoretical basis, there is no reason to expect accurate predictions of sweep efficiency, fluid injectivity, and phase properties, for example.

Phase-equilibrium calculations in compositional simulation consist of stability analysis and flash calculations. Stability analysis, if performed properly, can determine whether a phase is thermodynamically unstable. If that phase is unstable, a flash calculation is performed to obtain multiphase properties. The most common procedure for stability analysis is based on the stationary-point method of Michelsen (1982a). A widely used procedure for flash calculations is based on solution of fugacity equations for the traditional two-phase case and minimization of Gibbs free energy for a case of three or more phases (Michelsen 1982b). A flash calculation iteratively solves $N_C(N_P-1)$ equations, where $N_P$ is the number of phases and $N_C$ is the number of components used in the calculations. Stability analysis based on the stationary-point method iteratively solves $N_C$ equations. Therefore, phase-equilibrium calculations become more time-consuming as $N_C$ or $N_P$ increases. The increasing computational cost is a significant drawback of compositional simulation. Lumping detailed components into fewer grouped components can speed up the simulation by decreasing $N_C$ used in the calculations, but this often deteriorates the accuracy of phase-behavior predictions, which is important in gasflooding simulations. Using more components in reservoir simulation is also suitable for reservoir/surface integrated modeling because surface-process simulation typically requires 16–30 components (Leibovici et al. 2000).

A desirable approach to an efficient simulation is to decrease the computational time without loss of accuracy. A reduced method that originated with Michelsen (1986) has been studied as a potential solution. Variants of Michelsen's reduced flash were extended to handle nonzero binary interaction coefficients (Jensen and Fredenslund 1987; Hendriks 1988; Hendriks and van Bergen 1992; Kaul and Thrasher 1996; Li and Johns 2006). Other previous studies on reduced methods include comparisons of algorithms and application to stability analysis (Firoozabadi and Pan 2002; Nichita et al. 2002; Pan and Firoozabadi 2003; Hoteit and Firoozabadi 2006). Okuno et al. (2009a) developed robust and efficient algorithms for stability analysis and flash calculations using a reduced method for two hydrocarbon phases. They implemented the algorithms in a compositional simulator to demonstrate that their reduced method can decrease computational time significantly without loss of accuracy.

* Now with the Japan Petroleum Exploration Company.



Original SPE manuscript received for review 29 July 2009. Revised manuscript received for review 8 September 2009. Paper (SPE 125226) peer approved 28 September 2009.

| TABLE 1—PROPERTIES OF THE TERNARY MIXTURE | | | | | |
|---|---|---|---|---|---|
| | Mole Fraction (Mol %) | $T_c$ (°F) | $P_c$ (psia) | Acentric Factor | BIC* |
| $CO_2$ | 70 | 87.89 | 1,069.87 | 0.225 | 0.00 |
| $C_1$ | 20 | −116.59 | 667.20 | 0.008 | 0.12 |
| $n$-$C_{20}$ | 10 | 920.93 | 161.66 | 0.907 | 0.10 |

* All others are 0.0.

The studies on reduced methods that were mentioned assume that only two hydrocarbon phases exist. Nichita et al. (2006) extended a reduced method to more than two phases and reported calculation results and number of iterations in standalone calculations for three different fluids. They did not report the efficiency of their algorithm by comparing with other standard algorithms in terms of computational time. In this paper, we extend the algorithms of Okuno et al. (2009a) to three-phase calculations. We also implement them in an implicit-pressure/explicit-concentration (IMPEC) multiphase compositional reservoir simulator, UTCOMP (Chang et al. 1990), to demonstrate the improved efficiency and robustness compared to the original UTCOMP. To the best of our knowledge, this is the first time a reduced method is implemented in a compositional simulator capable of three-phase-equilibrium calculations.

In the following sections, we first demonstrate the importance of considering a third hydrocarbon phase in simulation of low-temperature gasfloods. Then, we present the formulation and algorithm for three-phase flash calculations using a reduced method. The algorithm is compared to a standard algorithm in terms of efficiency and robustness in standalone calculations. Last, we implement the algorithm in UTCOMP and give simulation case studies that demonstrate conclusively the efficiency and robustness of our reduced method.

## Importance of Considering Three-Phase Flash Calculations in Compositional Simulation

In this section, we demonstrate the importance of three-phase-equilibrium calculations in compositional simulation. We investigate difficulties with several procedures for two-phase-equilibrium approximations that have been proposed in the literature to avoid performing three-phase calculations.

**Use of Two-Phase Flash in a Three-Phase Region.** Nghiem and Li (1986) proposed to use only two-phase-equilibrium calculations to approximate complex reservoir simulations where three hydrocarbon phases can coexist. There are multiple solutions for a two-phase flash calculation in a three-phase region. For oleic ($L_1$), solvent-rich liquid ($L_2$), and gaseous ($V$) phases, a simple combinatorial analysis leads to three possible combinations; $L_1/L_2$, $L_1/V$, and $L_2/V$. However, the possibility of converging to $L_2/V$ is small because $L_2/V$ equilibrium occurs within a small region at very high solvent mole fractions on a pseudobinary pressure-concentration ($P$-$x$) diagram for oil and solvent. For example, $L_2/V$ equilibrium occurs for solvent mole fractions greater than 0.99 on the $P$-$x$ diagram studied by Turek et al. (1988). Therefore, a two-phase solution is likely to be $L_1/L_2$ or $L_1/V$.

Which of the two possible solutions is obtained by a two-phase flash calculation in the three-phase region depends on the overall composition. To see this, we consider a ternary mixture consisting of $CO_2$, $C_1$, and $n$-$C_{20}$. The properties of the ternary mixture are shown in **Table 1. Fig. 1** shows the tie-triangle at 40°F and 1,000 psia calculated by using the Peng-Robinson EOS (Peng and Robinson 1976). The three vertices represent fixed equilibrium compositions of the gaseous ($V$), oleic ($L_1$), and $CO_2$-rich liquid ($L_2$) phases. A false two-phase solution depends on the overall composition within the tie-triangle because there is one degree of freedom after temperature and pressure are specified.

We now perform a series of two-phase flash calculations with varying overall composition from Point A (0.655, 0.219) to Point C (0.737, 0.135), as shown in Fig. 1. The tie-line found by two-phase flash calculations at Point A must result in the $L_1/V$ phases because it lies on the boundary of the tie-triangle. For the same reason, the two-phase flash at Point C must result in $L_1/L_2$ phases. Thus, for flash calculations from Points A to C, there must be a composition that discontinuously changes from the $L_1/V$ tie-line to the $L_1/L_2$ tie-line. This is given by Point B in Fig. 1, where both intensive and extensive properties of the phases discontinuously change. For example, compressibility factors and phase mole fractions for the two phases are shown in **Fig. 2.** The compressibility factor of the gaseous phase exhibits a significant change from 0.474 to 0.208. To see the effect of the discontinuity on reservoir simulation, we calculate the saturation of phase $j$ as $S_j = \beta_j Z_j / \Sigma_i \beta_i Z_i$, where $i = 1, \ldots, N_P$ and $\beta_j$ and $Z_j$ are the phase mole fraction and compressibility factor of phase $j$, respectively. The variation of the oleic-phase saturation for the fictitious two-phase system is shown in **Fig. 3.** The oleic-phase saturation discontinuously varies from 0.55 to 0.70. Oscillations in physical properties caused by the discontinuous changes of flash-calculation solutions were observed by Khan

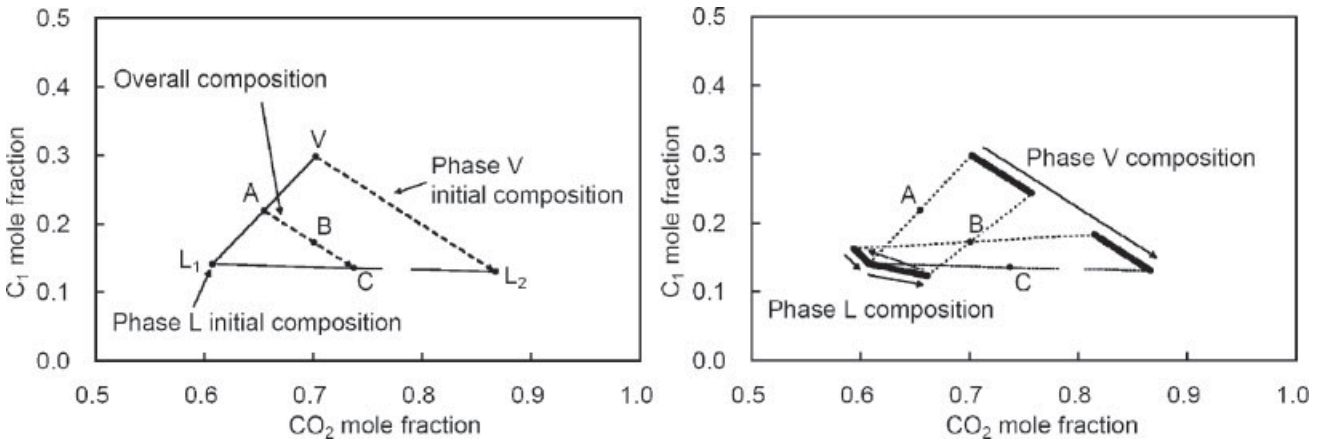


**Fig. 1—Tie-triangle for the ternary mixture given in Table 1 at 40°F and 1,000 psia using the Peng-Robinson EOS. Left: Overall compositions and initial estimates for two-phase flash calculations in the three-phase region. Right: Resulting two-phase flash calculations in the three-phase region for those overall compositions.**

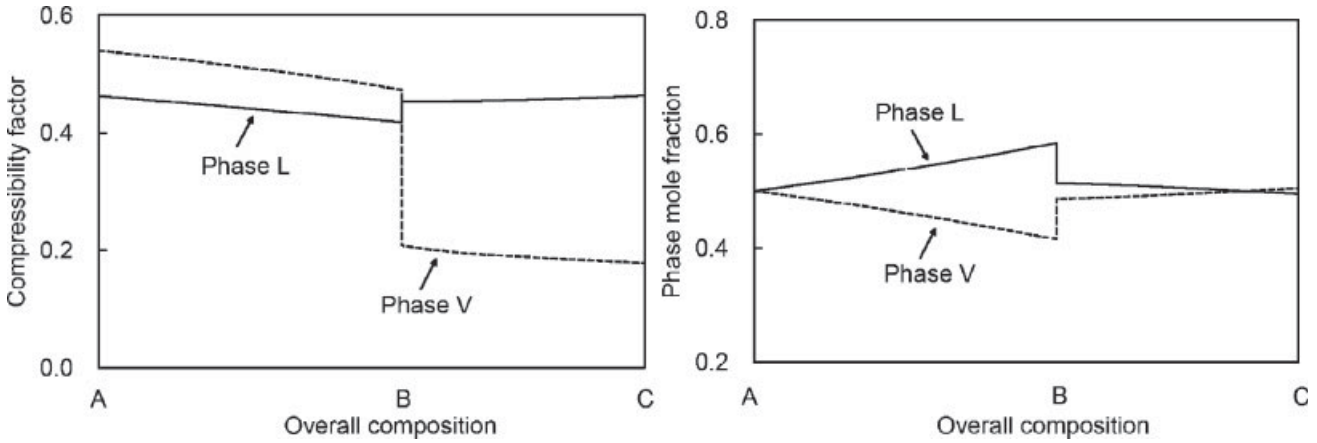


**Fig. 2—Left: Variation of compressibility factors for the two-phase solutions with changing overall composition from Composition A to C as shown in Fig. 1. Right: Variation of phase mole fractions for the two-phase solutions with changing overall composition.**

et al. (1992) in their simulations using only two-phase-equilibrium calculations in the three-phase region. The discontinuity also causes substantial reductions in timestep sizes and often stops the simulation from proceeding, as shown in Fig. 3.

Nghiem and Li (1986) attempted to select $L_1/L_2$ solutions during their simulations in the three-phase region by using initial estimates for $K$-values between the $L_1$ and $L_2$ phases from the previous timestep. However, if the overall composition is located between Point A and a point (0.696, 0.177) near Point B, the two-phase flash calculation converges to the $L_1/V$ solution even if the $K$-values between $L_1$ and $L_2$ are provided as the initial estimate. That is, their procedure does not guarantee avoidance of this discontinuity.

Two-phase flash calculations in a three-phase region can also be performed as a preconditioning step for three-phase flash calculations. However, stability analysis can provide a good initial estimate for subsequent three-phase flash calculations.

**Two-Phase EOS Representation of Three-Phase Behavior.** Fong et al. (1992) presented fluid-characterization procedures for a two-phase EOS model that can be used in reservoir simulation to approximate three-phase behavior of mixtures of $CO_2$ and low-temperature reservoir oil. Their fluid-characterization approach attempts to eliminate the three-phase region on the $P$-$x$ diagram for the oil and $CO_2$. Their motivation was that the approximation could avoid long computational time spent in phase-equilibrium calculations, convergence problems associated with three-phase flash calculations, and use of a four-phase relative permeability model. They compared two characterization procedures, which are different only in what portion of the $P$-$x$ diagram is matched by tuning binary interaction coefficients (BICs) of $CO_2$ to experimental data. Their first procedure, A, is to match the boundary between $L_1/V$ and $L_1$ at low $CO_2$ mole fractions. Their second procedure, B, is to match the boundary between $L_1/V$ and $L_1$ at high $CO_2$ mole fractions for a two-phase representation with the upper boundary of the $L_1/L_2/V$ region. Procedure B eliminates not only the $L_1/L_2/V$ region but also the $L_1/L_2$ region.

On the basis of the comparisons between Procedures A and B and slimtube data, they concluded that Procedure B is superior to Procedure A for approximating three-hydrocarbon-phase simulation. However, their procedure, although novel, has little theoretical basis and may provide inaccurate simulation results, such as sweep efficiency, fluid injectivity, and phase properties. For example, the recovery curves from their slim-tube simulations with the North Ward Estes (NWE) oil using Procedures A and B did not exhibit the sharp bend at breakthrough as observed in the slimtube test.

We demonstrate the use of their characterization procedures by considering 1D displacement of the NWE oil with impure $CO_2$, for which the component properties are taken from Khan et al. (1992), as shown in **Table 2. Fig. 4** shows the predicted $P$-$x$ diagram at the reservoir temperature of 83°F and the three-phase region on the pressure/temperature ($P$-$T$) diagram at several oil and gas mixtures. In the $P$-$x$ diagram, an $L_1/L_2/V$ region exists between 1,050 and 1,350 psia at solvent mole fractions greater than 0.65. The critical point of the injection gas is 81°F and 1,115 psia, and there is no phase boundary at the reservoir temperature of 83°F for the injection gas (i.e., at the solvent mole fraction of 1.0 in the $P$-$x$ diagram). The $P$-$T$ diagram shows that the maximum temperature for existence of the three-phase region is 93°F at a solvent mole fraction of 0.90.

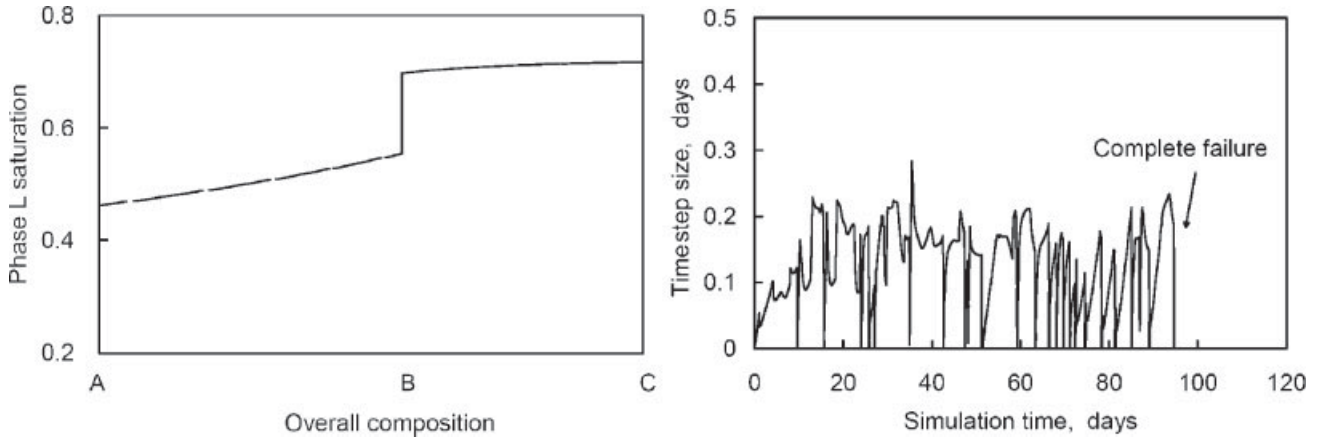


**Fig. 3—Left: Variation of saturation for Phase L with changing overall composition assuming two-phase equilibrium. Right: Timestep-size behavior during a simulation using only two-phase flash calculations in the three-phase region.**

**TABLE 2—FLUID PROPERTIES FOR SIMULATIONS WITH THE NWE OIL***

| | Oil (Mol %) | Gas (Mol %) | Molecular Weight | $T_C$ (°F) | $P_C$ (psia) | Acentric Factor | BIC** $CO_2$ | $h$ | $g$ |
|---|---|---|---|---|---|---|---|---|---|
| $CO_2$ | 0.77 | 95.0 | 44.01 | 87.89 | 1069.87 | 0.225 | 0.00 | 1.0 | 1.00 |
| $C_1$ | 20.25 | 5.0 | 16.04 | –116.59 | 667.20 | 0.008 | 0.12 | 0.0 | 0.12 |
| $C_{2–3}$ | 11.80 | 0.0 | 38.40 | 158.88 | 653.37 | 0.130 | 0.12 | 0.0 | 0.12 |
| $C_{4–6}$ | 14.84 | 0.0 | 72.82 | 379.87 | 485.94 | 0.244 | 0.12 | 0.0 | 0.12 |
| $C_{7–14}$ | 28.63 | 0.0 | 135.82 | 625.86 | 351.54 | 0.600 | 0.09 | 0.0 | 0.09 |
| $C_{15–24}$ | 14.90 | 0.0 | 257.75 | 861.15 | 261.51 | 0.903 | 0.09 | 0.0 | 0.09 |
| $C_{25+}$ | 8.81 | 0.0 | 479.95 | 1202.09 | 250.31 | 1.229 | 0.09 | 0.0 | 0.09 |

* From Khan et al. (1992)
** All others are 0.0.

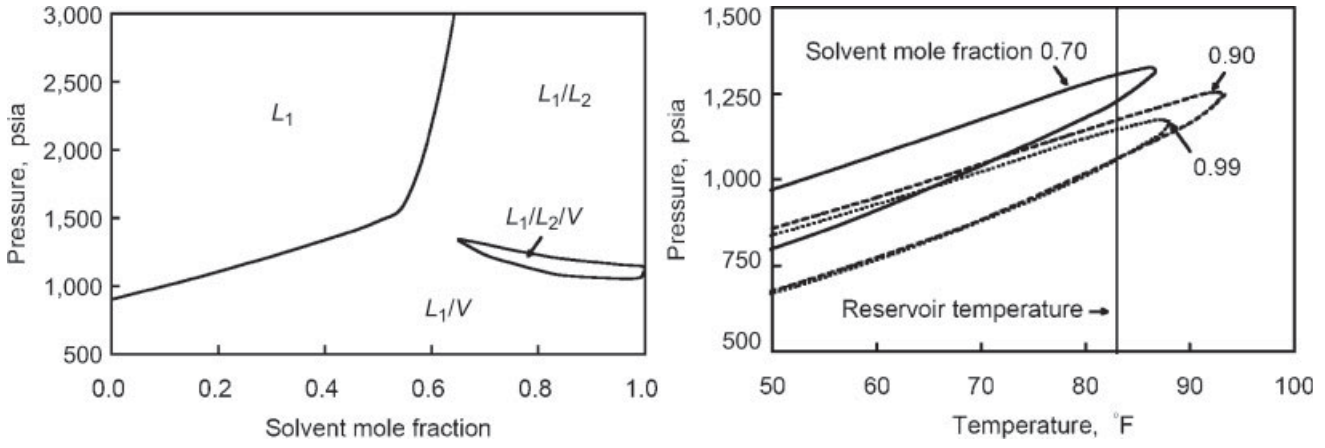


**Fig. 4—Left: *P-x* diagram at 83°F for the NWE oil and injection gas (solvent) given in Table 2. Right: *P-T* diagrams for mixtures of the NWE oil and injection gas given in Table 2 for different oil/gas mixtures.**

Starting with the original fluid characterization shown in Table 2, we obtain the following BICs of $CO_2$ by using Procedure A: 0.2 for $CO_2/C_1$, $CO_2/C_{2–3}$, $CO_2/C_{4–6}$, and $CO_2/C_{7–14}$ and 0.0 for $CO_2/C_{15–24}$ and $CO_2/C_{25+}$. The *P-x* diagram at 83°F using Procedure A is compared with the original in **Fig. 5.** The boundary between $L_1/V$ and $L_1$ at low solvent mole fractions is almost identical with the original. Fig. 5 also shows the three-phase region on the *P-T* diagram at different solvent mole fractions. Because the three-phase envelopes do not intersect the reservoir temperature of 83°F, there are no three-phase regions in the *P-x* diagram at 83°F. Changes in BICs of $CO_2$ affect the phase-behavior predictions of oil very little because $CO_2$ mole fraction is small in the oil. For example, **Fig. 6** shows that the *P-T* diagram from the original characterization coincides with that from Procedure A.

Reservoir properties for the 1D simulation are shown in **Table 3.** An injector at the first cell is operated at a constant injection rate of 750 scf/D, and a producer at the last cell produces at a constant bottomhole pressure of 900 psia. The total variation diminishing higher-order scheme of Liu et al. (1994) in UTCOMP is used to control numerical dispersion in our simulations.

Fig. 6 shows the recoveries using the original fluid characterization of Khan et al. (1992) and Procedure A. The former is 27% higher than the latter after 2.0 hydrocarbon pore volumes injected (HCPVI). That is, displacement efficiency can be underestimated

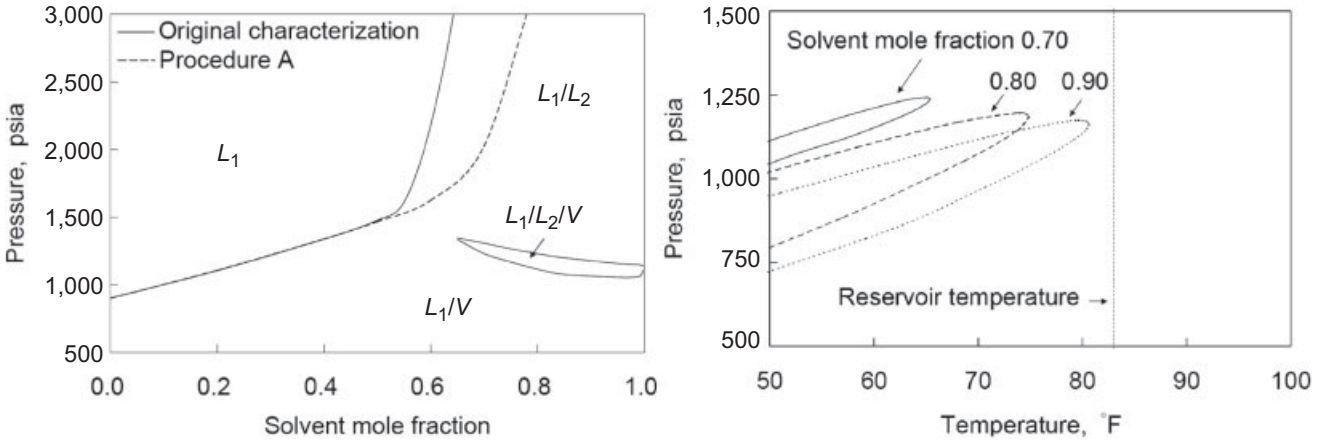


**Fig. 5—Left: Comparison of *P-x* diagram at 83°F from Procedure A with that from the original characterization for the NWE oil and injection gas (solvent) given in Table 2. Right: *P-T* diagrams at different mixing ratios of the NWE oil and injection gas using Procedure A.**

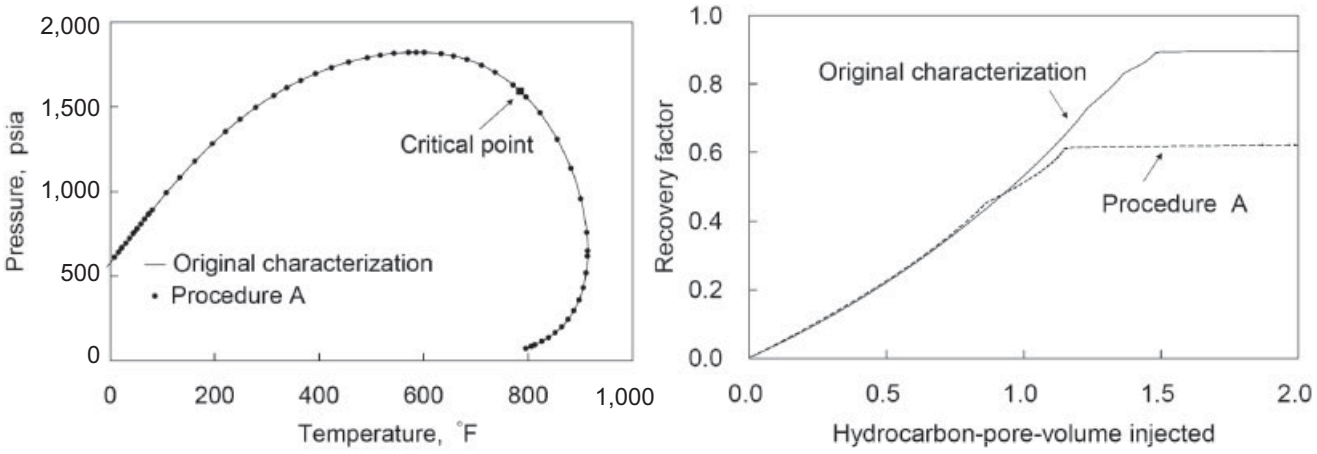


**Fig. 6—Left: Comparison of *P-T* diagram from Procedure A with that from the original characterization for the NWE oil. Right: Recoveries for 1D simulations with characterization Procedure A and the original characterization for the NWE oil.**

**TABLE 3—RESERVOIR PROPERTIES FOR 1D SIMULATION WITH THE NWE OIL**

| | |
|---|---|
| Dimensions | 500×5×10 ft |
| Number of grid cells | 100×1×1 |
| Porosity | 0.15 |
| Permeability | 30 md |
| Initial pressure | 1,000 psia |
| Reservoir temperature | 83 °F |
| Relative permeability model | Corey |
| Residual saturation ($W/L_1/G/L_2$*) | 0.4/0.2/0.05/0.05 |
| Endpoint relative permeability ($W/L_1/G/L_2$*) | 0.35/0.50/0.65/0.65 |
| Exponent ($W/L_1/G/L_2$*) | 3.0/3.0/3.0/3.0 |
| Initial saturation ($W/L_1/G/L_2$*) | 0.4/0.6/0.0/0.0 |

*$W$: aqueous phase; $L_1$: oleic phase; $G$: gaseous phase; $L_2$: $CO_2$-rich liquid phase.

significantly when Procedure A is used. Also, Procedure A does not necessarily avoid the three-phase calculations, as was originally assumed by Fong et al. (1992). When we allow for three-phase-equilibrium calculations in the simulation with Procedure A, three hydrocarbon phases exist over a few consecutive grid cells near the displacement front during the simulation. This is because Procedure A attempts to eliminate a three-phase region only on a *P-x* diagram, which represents phase behavior along the mixing line between the oil and injection gas, instead of the actual composition path observed during the displacement. As long as three-phase regions exist and only two-phase-equilibrium calculations are performed in the simulation, convergence problems can stop the simulation from proceeding as discussed in the previous section, even though convergence problems do not occur in this particular case. Therefore, Procedure A leads either to a complete failure of simulation or to erroneous simulation results.

We now consider Procedure B by starting with the original characterization in Table 2. We could not, however, achieve a good match using Procedure B. Although Fong et al. (1992) were able to apply the procedure starting with a different fluid characterization, there are no EOS parameters presented in their paper. Procedure B likely cannot be applied in some situations because, as described later, it requires a significant deviation from the original characterization for three-phase behavior.

**Fig. 7** shows projections of the *P-T-x* diagram onto *P-T* and *T-x* diagrams for the pseudobinary mixture of the NWE oil and

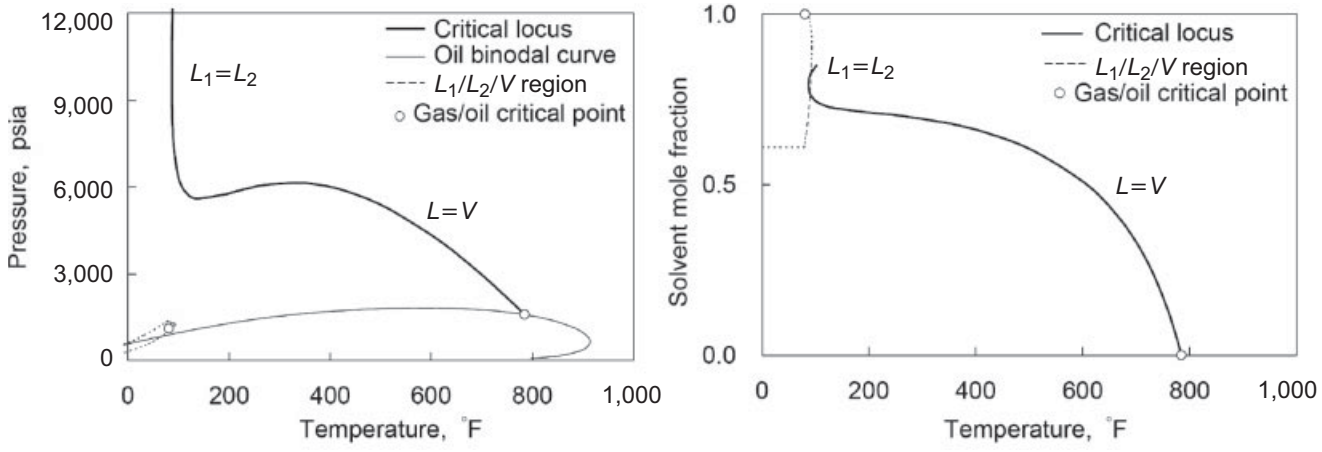


**Fig. 7—*P-T* and temperature/concentration (*T-x*) projections of the pressure/temperature/concentration (*P-T-x*) diagram for the pseudobinary mixture of the NWE oil and injection gas given in Table 2.**

injection gas. On the *P-T* diagram, the binodal curve for 100% oil is shown, but that for 100% gas is not shown for clarity. On the *T-x* diagram, the critical locus up to 22,938 psia at a solvent mole fraction of 0.85 is shown. This type of phase behavior in Fig. 7 is analogous to that for binary systems $CO_2$+*n*-alkane from *n*-$C_{14}$ through *n*-$C_{21}$ in that $L_1/L_2/V$ equilibrium exists and the critical locus of $L = V$ critical points gradually changes its behavior to $L_1 = L_2$ (Alwani and Schneider 1976; Miller and Luks 1989). Procedure B attempts to obtain phase behavior similar to binary systems $CO_2$+*n*-alkane from $C_1$ through *n*-$C_6$, which exhibit a continuous $L = V$ critical locus between two critical points for the pure components with neither $L_1/L_2/V$ nor $L_1/L_2$ equilibrium. The former type of phase behavior is categorized as Type III and the latter as Type I, according to van Konynenburg and Scott (1980), who introduced the classification of fluid-phase behavior for binary mixtures on the basis of the van der Waals EOS. The difference between the phase-behavior types for $CO_2$+*n*-alkane binary systems comes from the difference in the carbon number or chain length of the *n*-alkane molecule. Considering that the NWE oil contains a large amount of components with much larger carbon numbers than *n*-$C_6$, Procedure B should be difficult to apply to the NWE oil.

## Reduced Method for Three-Phase Flash Calculations

Three-phase-equilibrium calculations are important in simulation of low-temperature gasfloods. However, the computational time required and robustness of the calculations have led several authors to make two-phase-equilibrium approximations. The use of a reduced method is a potential practical solution. For miscible-gas simulations involving only *L*/*V* equilibrium, Okuno et al. (2009a) demonstrated that a reduced method gives significant savings in computational time with improved robustness. In this section, we extend their reduced flash algorithm to three-phase calculations. We use the same stability analysis algorithm as in Okuno et al. (2009a) because stability analysis is performed only on a single-phase mixture or one of the individual phases of a multiple-phase mixture (Perschke et al. 1989).

In this section, we first present the reduced parameters used in this method. We then derive the formulation for $N_P$-phase flash calculations using the reduced method and present an algorithm to solve the formulated problem. We also compare the efficiency and robustness of the reduced flash with those of the minimization of the Gibbs free energy of Perschke et al. (1989) for three-phase standalone calculations.

**Reduced Parameters.** The Peng-Robinson EOS is used with the van der Waals mixing rules throughout this paper, although any cubic EOS can be used. To handle nonzero BICs, Li and Johns (2006) introduced two sets of component-specific parameters, $h_i$ and $g_i$, to replace BICs: $k_{ij} = (h_i - h_j)^2 g_i g_j$, where $i, j = 1, \ldots, N_C$. The parameters $h_i$ and $g_i$ can be considered as fitting parameters to represent the BICs or, better yet, to match pressure/volume/temperature (*PVT*) data directly. As long as the characterized fluid model using the parameters $h_i$ and $g_i$ can predict the phase behavior accurately, the reduced phase-equilibrium calculations are as accurate as the conventional calculations. The reduced parameters are defined as

$$\theta_{kj} = \sum_{i=1}^{N_C} \eta_{ki} x_{ij} , \quad \ldots\ldots\ldots\ldots\ldots\ldots\ldots\ldots\ldots\ldots\ldots\ldots\ldots\ldots (1)$$

$$\text{where } \eta_i = \left(B_i, \sqrt{A_i}, \sqrt{A_i} h_i g_i, \sqrt{A_i} h_i^2 g_i, \sqrt{A_i} g_i\right), j = 1,\ldots,N_P$$

and $k = 1, \ldots, 5$.

Fugacity coefficients for a phase can be expressed as functions of the five reduced parameters for the corresponding phase. As described later, the number of independent variables for the reduced flash is $6(N_P-1)$ compared to $N_C(N_P-1)$ for the conventional flash calculations. That is, the number of equations to be solved in the reduced flash does not depend on $N_C$ used in the calculations. Therefore, the reduced flash can decrease the number of equations to be solved when more than six components are used in the calculations. This is often the case in compositional simulation, especially when the phase behavior is complex.

The reduced number of equations can be exploited when Newton's method is used as the solution technique. In this research, the reduced method is initiated by the conventional successive substitution (SS) both for stability analysis and for flash calculations and is followed by Newton's method. Use of SS first and Newton's method next is commonly applied in compositional reservoir simulation because Newton's method converges quadratically only when a good initial estimate of the parameters is given. SS is linearly convergent within a larger region of convergence compared to Newton's method.

An alternative procedure to obtain reduced parameters is to approximate a BIC matrix using the spectral expansion (Hendriks and van Bergen 1992). In a reduced method based on the spectral expansion, the minimum number of reduced parameters for accurate phase-behavior predictions depends on the values of BICs as shown by Firoozabadi and Pan (2002). Nichita et al. (2006) stated that a reduced method using the spectral expansion is effective only if a BIC matrix has only few nonzero eigenvalues. The reduced method using the parameters of Li and Johns (2006) is more accurate than that using the spectral expansion because parameters $h$ and $g$ for the former can be used directly in EOS fluid characterization to match *PVT* data. Although we use the reduced parameters of Li and Johns (2006) in this paper, the solution techniques for a reduced method presented in this paper and Okuno et al. (2009a) can also be applied using reduced parameters from the spectral expansion.

**Three-Phase Flash Calculations Using a Reduced Method.** For a flash calculation at a given temperature and pressure, the solution must be the global minimum of the Gibbs free energy in composition space. The first-order necessary condition for a minimum of the Gibbs free energy leads to the following fugacity equations:

$$F_{ij} = \ln x_{ij}\varphi_{ij} - \ln x_{iN_P}\varphi_{iN_P} = 0 , \quad \ldots\ldots\ldots\ldots\ldots\ldots\ldots\ldots (2)$$

where $i = 1,\ldots,N_C$ and $j = 1,\ldots,(N_P-1)$.

In Eq. 2, phase $N_P$ is the reference phase. The fugacity equations must be satisfied with the following material-balance equations:

$$z_i = \sum_{j=1}^{N_P} \beta_j x_{ij} , \ \sum_{j=1}^{N_P} \beta_j = 1 , \text{ and } \sum_{i=1}^{N_C} x_{ij} = 1 , \quad \ldots\ldots\ldots (3)$$

where $i = 1,\ldots,N_C$ and $j = 1,\ldots,N_P$.

We define $K_{ij} = x_{ij}/x_{iNP}$ for $i = 1, \ldots, N_C$ and $j = 1, \ldots, (N_P-1)$. Nghiem and Li (1984) solved Eqs. 2 and 3 for $2N_C$ independent variables, $\ln K_{i1}$ and $\ln K_{i2}$ ($i = 1, \ldots, N_C$), for their three-phase flash calculations. Rearranging Eq. 2, *K*-values become functions of $5N_P$ reduced parameters.

$$K_{ij} = \varphi_{iN_P}\left(\underline{\theta}_{N_P}\right)/\varphi_{ij}\left(\underline{\theta}_j\right) , \quad \ldots\ldots\ldots\ldots\ldots\ldots\ldots\ldots (4)$$

where $i = 1,\ldots,N_C$ and $j = 1,\ldots,(N_P-1)$.

Considering Eq. 3, the reduced parameters for the reference phase $N_P$ can be expressed using reduced parameters and phase mole fractions for the other $(N_P-1)$ phases.

$$\theta_{kN_P} = \left(\theta_k^z - \sum_{j=1}^{N_P-1} \beta_j \theta_{kj}\right)/\beta_{N_P} , \quad \ldots\ldots\ldots\ldots\ldots\ldots (5)$$

where $\theta_k^z = \sum_{i=1}^{N_C} \eta_{ki} z_i$ and $k = 1,\ldots,5$.

Then, *K*-values in Eq. 3 can be considered as functions of $6(N_P-1)$ variables. Once *K*-values are calculated, phase compositions are computed directly as

$$x_{iN_P} = z_i/t_i \text{ and } x_{ij} = K_{ij} x_{iN_P} , \quad \ldots\ldots\ldots\ldots\ldots\ldots\ldots (6)$$

where $t_i = 1 - \left[\sum_{j=1}^{N_P-1}\left(1-K_{ij}\right)\beta_j\right]$, $i = 1,...,N_C$ and $j = 1,...,\left(N_P-1\right)$. The rearrangement of the original flash formulation confirms that phase properties can be viewed as functions of $6(N_P-1)$ independent variables $\theta_{kj}$ and $\beta_j$, where $k$ = 1, …, 5 and $j$ = 1, …, $(N_P-1)$.

The reduced flash equations to be solved for the $6(N_P-1)$ independent variables are

$$F_m^R = \theta_{kj} - \sum_{i=1}^{N_C}\eta_{ki}x_{ij} = 0 \quad \text{for } m = k \times j$$

and

$$F_m^R = \sum_{i=1}^{N_C}\left(x_{iN_P} - x_{ij}\right) = 0 \quad \text{for } m = 5\left(N_P-1\right)+j, \quad \ldots\ldots\ldots (7)$$

where $k$ = 1, …, 5 and $j$ = 1, …, $(N_P-1)$. Eq. 7 includes the multiphase Rachford-Rice equations (Rachford and Rice 1952) to satisfy the material-balance equations. The Jacobian matrix is of size $6(N_P-1)\times 6(N_P-1)$, independent of $N_C$ used in the calculation.

The algorithm to solve Eq. 7 is an extension of the algorithm of Okuno et al. (2009a) for two-phase calculations. The reduced flash starts with an initial estimate from the conventional SS. The algorithm is the following:

1. Calculate $\theta_k^z$ ($k$ = 1, ..., 5) as defined in Eq. 5.
2. Obtain initial estimates for the $6(N_P-1)$ independent variables, $\theta_{kj}$ and $\beta_j$ ($k$ = 1, …, 5 and $j$ = 1, …, $N_P-1$), based on the solution from SS and Eq. 1.
3. Calculate the reduced parameters for the reference phase $N_P$ using Eq. 5.
4. Calculate compressibility factors and fugacity coefficients for the $N_P$ phases using an EOS. When the cubic EOS has multiple roots of the compressibility factor, the correct root is selected that results in the lowest Gibbs free energy (Evelein et al. 1976).
5. If $\max_{ij}\{|F_{ij}|\} < \varepsilon$, then stop. Otherwise, continue to Step 6.
6. Calculate $K$-values using Eq. 4 on the basis of the fugacity coefficients in Step 4.
7. Calculate compositions for the $N_P$ phases using Eq. 6.
8. Calculate the residuals of Eq. 7.
9. Construct the $6(N_P-1)\times 6(N_P-1)$ Jacobian matrix analytically [see Okuno (2009)] and solve the system of equations.
10. Update the $6(N_P-1)$ independent variables $\theta_{kj}$ and $\beta_j$ ($k$ = 1, …, 5 and $j$ = 1, …, $N_P-1$).
11. Repeat Steps 3, 4, and 6 to obtain a new set of $K$-values.
12. Solve the multiphase Rachford-Rice equations to obtain phase compositions, $x_{ij}$, and mole fractions, $\beta_j$ ($i$ = 1, …, $N_C$ and $j$ = 1, …, $N_P$), using the algorithm of Okuno et al. (2009b).
13. Update the independent variables $\theta_{kj}$ and $\beta_j$ ($k$ = 1, …, 5 and $j$ = 1, …, $N_P-1$) using Eq. 1.
14. Go to Step 3.

The preceding algorithm updates the independent variables twice during one iteration. The first update is Newton's method, and the second is an SS step (Steps 11 through 13). This additional SS step is also used by Okuno et al. (2009a) only for extremely difficult cases for a two-phase flash where overall compositions are very near the binodal curve in the critical region. We recommend that it always be used for three-phase calculations.

The stopping criterion for the algorithm is based on the fugacity equations, Eq. 2, instead of the RF equations, Eq. 7, because the scale of the residual for Eq. 2 can be significantly different from that of Eq. 7. The criterion based on the fugacity equations is thermodynamically more fundamental than that based on the RF equations, Eq. 7.

## Standalone Three-Phase Flash Calculations

We now demonstrate the efficiency and robustness of the RF algorithm for three-phase calculations. We compare the RF algorithm with the method of minimization of the Gibbs free energy (MG) of Michelsen (1982b), which was implemented in UTCOMP by Perschke et al. (1989). MG minimizes the Gibbs free energy in terms of $N_C(N_P-1)$ component mole numbers of the independent phases. The algorithm is based on Newton's method with a line-search technique, where the modified Cholesky decomposition algorithm of Gill and Murray (1974) provides a search direction if the Hessian matrix is not positive definite.

Conventional two-phase flash calculations use root-finding of fugacity equations instead of MG. MG, however, is used for our comparisons for three-phase flash calculations because of the robustness and computational efficiency. MG is more robust than root-finding of fugacity equations because MG can ensure that the Gibbs free energy is decreased in each iteration step. Okuno et al. (2009a) showed that MG can take shorter computational time per iteration than root-finding of fugacity equations for two-phase flash calculations using 10 or more components. Michelsen (1982b) recommended using MG for more than two phases, instead of root-finding of fugacity equations.

We consider a flash calculation for a mixture of the Bob Slaughter Block (BSB) oil and impure $CO_2$. A fluid model was developed by Khan et al. (1992) using the Peng-Robinson EOS, as shown in **Table 4.** For this example flash calculation, the temperature and pressure are 105°F and 1,295 psia. **Table 5** gives the overall composition, which is a mixture of the oil and injection gas given in Table 4. The calculation starts with stability analysis for a single-phase mixture. After the stability analysis detects an instability, a two-phase flash calculation is performed to obtain an intermediate two-phase solution. Stability analysis is performed again for one of the two phases. The three-phase flash is performed when this stability analysis determines that the intermediate two-phase system is unstable. The stability analysis also provides an initial estimate for the following three-phase flash with the conventional SS. SS is switched to Newton's method for either the RF algorithm or MG when $\max_{ij}\{|F_{ij}|\} < 10^{-3}$.

This example flash calculation is a difficult case close to a critical point. Table 5 gives the three-phase solution for this problem. The resulting equilibrium compositions for the oleic and $CO_2$-rich liquid phases are near each other, indicating that the conditions are in a near-critical region. **Fig. 8** shows the convergence behaviors of the RF algorithm and MG for this example calculation. MG takes 17 iterations to satisfy the stopping criterion of $\max_{ij}\{|F_{ij}|\} < 10^{-8}$ compared to 10 iterations for the RF algorithm. The slow convergence of the initial iterations for both algorithms indicates that the switching point from SS to Newton's method is not sufficiently

**TABLE 4—FLUID PROPERTIES FOR SIMULATIONS WITH THE BSB OIL***

| | Oil (Mol %) | Gas (Mol %) | Molecular Weight | $T_C$ (°F) | $P_C$ (psia) | Acentric Factor | BIC** $CO_2$ | $h$ | $g$ |
|---|---|---|---|---|---|---|---|---|---|
| $CO_2$ | 3.37 | 95.0 | 44.01 | 87.89 | 1,069.87 | 0.2250 | 0 | 1.0 | 1.000 |
| $C_1$ | 8.61 | 5.0 | 16.04 | −171.67 | 667.20 | 0.0080 | 0.055 | 0.0 | 0.055 |
| $C_{2-3}$ | 15.03 | 0.0 | 37.20 | 159.90 | 652.56 | 0.1305 | 0.055 | 0.0 | 0.055 |
| $C_{4-6}$ | 16.71 | 0.0 | 69.50 | 374.13 | 493.07 | 0.2404 | 0.055 | 0.0 | 0.055 |
| $C_{7-15}$ | 33.04 | 0.0 | 140.96 | 630.68 | 315.44 | 0.6177 | 0.105 | 0.0 | 0.105 |
| $C_{16-27}$ | 16.11 | 0.0 | 280.99 | 892.16 | 239.90 | 0.9566 | 0.105 | 0.0 | 0.105 |
| $C_{28+}$ | 7.13 | 0.0 | 519.62 | 1,236.79 | 238.12 | 1.2683 | 0.105 | 0.0 | 0.105 |

* From Khan et al. (1992)
** All others are 0.0.

| TABLE 5—THREE-PHASE SOLUTION FOR AN EXAMPLE FLASH CALCULATION WITH THE BSB OIL | | | | | |
|---|---|---|---|---|---|
| | | Overall composition | Oleic phase | Gaseous phase | $CO_2$-rich liquid phase |
| Phase mole fractions | | | 0.62169 | 0.17728 | 0.20103 |
| Component mole fractions | $CO_2$ | 0.57529 | 0.53522 | 0.74337 | 0.55099 |
| | $C_1$ | 0.07305 | 0.05410 | 0.15894 | 0.05592 |
| | $C_{2-3}$ | 0.10297 | 0.10873 | 0.07527 | 0.10957 |
| | $C_{4-6}$ | 0.09088 | 0.10614 | 0.02086 | 0.10546 |
| | $C_{7-15}$ | 0.10509 | 0.12903 | 0.00155 | 0.12236 |
| | $C_{16-27}$ | 0.03792 | 0.04750 | $6.2515\times10^{-6}$ | 0.04173 |
| | $C_{28+}$ | 0.01480 | 0.01928 | $9.0351\times10^{-10}$ | 0.01399 |

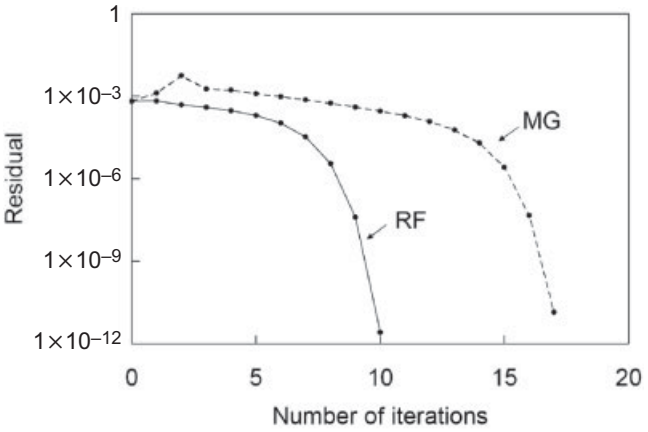


**Fig. 8—Convergence behaviors of the RF algorithm and the MG for an example of a three-phase calculation.**

close to the solution to exhibit a second-order convergence rate. This convergence behavior is characteristic of phase-equilibrium calculations near a critical point. The simple algorithm for RF exhibits remarkably improved convergence behavior compared to MG, which uses globally convergent techniques such as line search to enhance its convergence.

Total computational time of a flash calculation is determined by the number of iterations multiplied by the computational time per iteration. The RF algorithm generally takes fewer iterations compared to MG, as shown previously and by Okuno et al. (2009a).

We next compare computational time per iteration for the RF algorithm with that for MG. Computations are performed using a Pentium 4 processor running at 3.0 GHz and 2.0 GB of RAM throughout this research. The computational time per iteration depends on how close the current iteration point is to the solution because both the RF algorithm and MG contain an inner iteration loop; RF iteratively solves the Rachford-Rice equations, and MG performs line-search in an iterative manner inside the outer iteration loop. **Fig. 9** shows computational time per iteration for the RF algorithm and MG for different $N_C$. When more than seven components are used, the heaviest component is split to as many components as needed with the same properties. This is also true for the simulation case studies to be presented later. The left and right plots of Fig. 9 give the time per iteration when switched from SS with a criterion of $10^{-3}$ and $10^{-7}$, respectively. For both cases, the RF algorithm is faster than MG, and the advantage of the RF algorithm over MG becomes more significant as $N_C$ is increased. For the former case, the speed-up factor is 2.2 for 10 components and 6.3 for 20 components. For the latter case, the speed-up factor is 2.0 for 10 components and 4.7 for 20 components. Those speed-ups of the RF algorithm come from the reduced number of equations to be solved. For three phases, the number of equations is always 12 for the RF algorithm and $2N_C$ for MG.

As long as equality $k_{ij} = (h_i - h_j)^2 g_i g_j$ holds, the reduced method gives exactly the same calculation results as a conventional method using binary interaction coefficients. This fact does not depend on the number of components used. Tables 2 and 4 show that the equality holds for both the NWE and BSB oils. That is, the calculation results from the RF algorithm are the same as those from MG in the example calculations presented in this paper if the algorithms converge to the correct solution.

## Simulation Case Studies With the Reduced Method

We implemented and tested our algorithm for the reduced method in various runs with UTCOMP to confirm its robustness and efficiency. Two simulation examples are presented in this section.

UTCOMP is an IMPEC multiphase compositional simulator originally developed by Chang et al. (1990). Perschke et al.

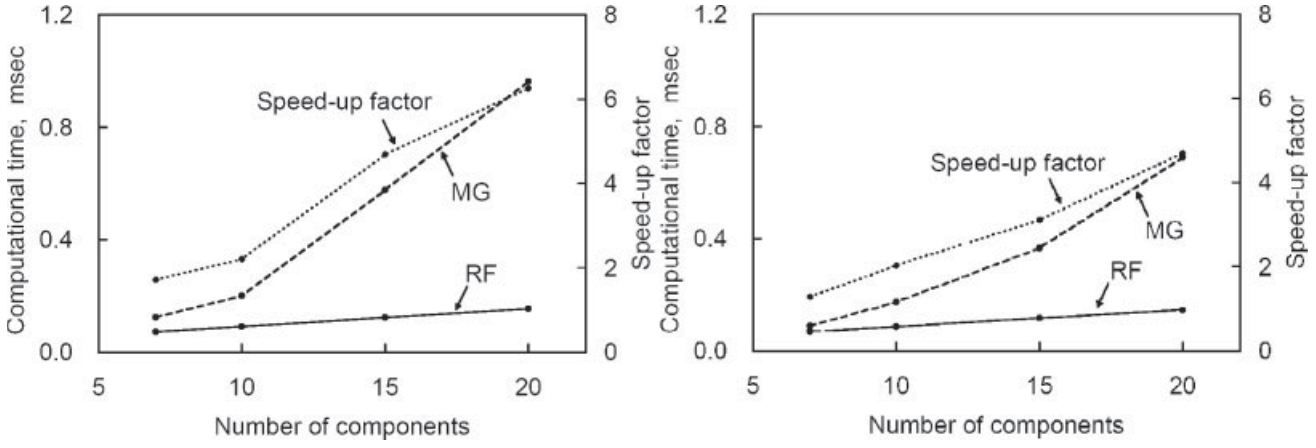


**Fig. 9—Comparisons of computational time per iteration for three-phase flash calculations using the RF algorithm and MG. Left: When SS is switched to either the RF algorithm or MG with a switching criterion of $\max_{ij}\{|F_{ij}|\} < 10^{-3}$. Right: When SS is switched to either the RF algorithm or MG with a switching criterion of $\max_{ij}\{|F_{ij}|\}<10^{-7}$.**

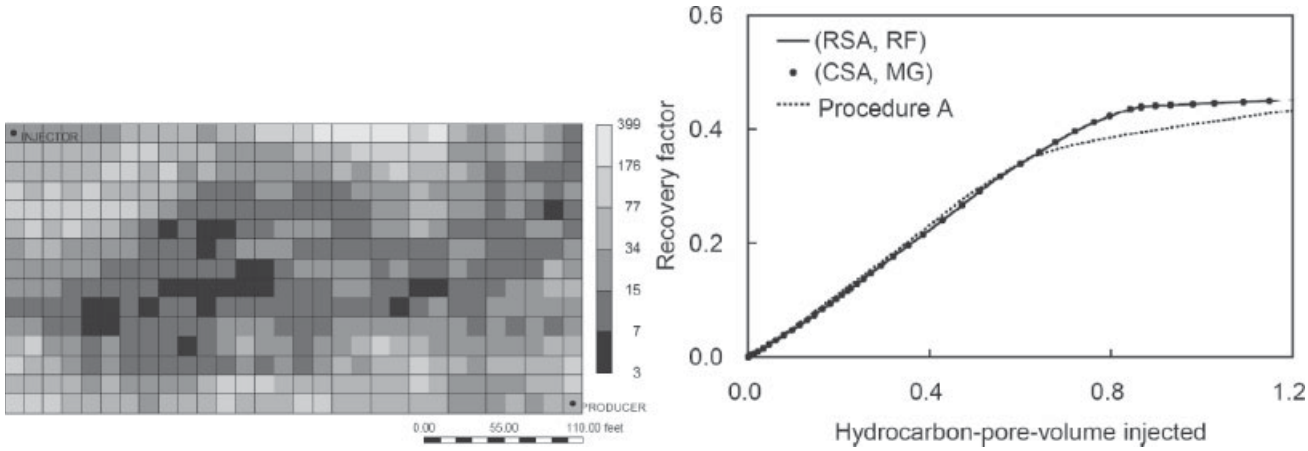


**Fig. 10—Left: Permeability field for the simulation case study with the NWE oil in millidarcies. Right: Recovery factors for cases (RSA, RF) and (CSA, MG) are almost identical to each other but are different from that with Procedure A.**

(1989) developed the phase-equilibrium algorithms in the original UTCOMP. The multiphase-equilibrium calculations in UTCOMP consist of stability analysis and flash calculations, for which a flow chart is given in Appendix A. The algorithms use accelerated SS and minimization of the Gibbs free energy for flash calculations and use the stationary-point method and minimization of the tangent plane distance function for stability analysis (Michelsen 1982a). All the calculations with the original UTCOMP are performed in conventional $N_C$ space instead of in reduced space. In this research, we replace the accelerated SS with the normal SS to start the second-order convergence method robustly. We also replace the original Rachford-Rice algorithm in UTCOMP with that given by Okuno et al. (2009b) because their algorithm is guaranteed to converge to the correct solution for any number of phases.

Stability analysis in UTCOMP is based on the procedure of Michelsen (1982a) as implemented by Perschke (1988). *K*-values from Wilson's correlation (1969) are used to generate two-sided initial phase compositions (i.e., vapor-like and liquid-like compositions) for stability analysis from one to two phases. For stability analysis from two to three phases, four initial estimates are used as is explained in Perschke (1988).

We compare the efficiency and robustness of the reduced method with those of the original code in UTCOMP for simulations with different fluids, numbers of components, and reservoir models. The reduced method uses the algorithms for reduced stability analysis (RSA) and RF calculations developed in this paper and by Okuno et al. (2009a). The original UTCOMP uses the conventional stability analysis (CSA) based on the stationary-point method and MG for flash calculations, both in conventional $N_C$ space. In those calculations, the conventional SS initiates the second-order convergence methods. The switching criteria from SS to the second-order convergence methods are $\max\{|S_i|\} < 10^{-3}$ for stability analysis and $\max_{ij}\{|F_{ij}|\} < 10^{-3}$ for flash calculations, where $S_i$ is stationarity equations to be satisfied at a stationary point of the tangent plane distance function (Michelsen 1982a) and $F_{ij}$ is defined in Eq. 2. The stopping criteria are $\max\{|S_i|\} < 10^{-8}$ for stability analysis and $\max_{ij}\{|F_{ij}|\} < 10^{-8}$ for flash calculations. In addition, CSA and MG use a relative step-size criterion, $\max\{|\delta\alpha_i/\alpha_i|\} < 10^{-8}$, where $\alpha_i$ is the $i$th independent variable and $\delta\alpha_i$ is the updated amount for $\alpha_i$.

Stability analysis for a single-phase mixture is performed in all single-phase grid cells. Flash calculations are performed only for grid cells where phase instability is detected by stability analysis. The Corey model is used for the relative permeability function. The parameters for relative permeability of a solvent-rich liquid phase are assumed to be the same as those of a gaseous phase. An aqueous phase exists at its residual saturation. The total variation diminishing higher-order scheme of Liu et al. (1994) is used to control numerical dispersion.

**NWE Oil With an Areal 2D Reservoir Model.** We consider an oil displacement with an injection gas consisting of 5% $C_1$ and 95% $CO_2$ for 1.2 HCPVI in a quarter of a staggered-line-drive pattern. The permeability field is stochastically generated for an areal, 2D reservoir model as shown in **Fig. 10.** The reservoir oil is the NWE oil for which a fluid model using the Peng-Robinson EOS was developed by Khan et al. (1992). The properties of the oil and injection gas are shown in Table 2. The MMP with pure $CO_2$ was experimentally determined to be 937 psia at the reservoir temperature of 83°F (Fong et al. 1992). Fig. 4 shows the *P-x* diagram for the reservoir oil and injection gas at the reservoir temperature predicted by the EOS model. **Table 6** gives the reservoir properties.

**TABLE 6—RESERVOIR PROPERTIES FOR THE SIMULATION CASE STUDY WITH THE NWE OIL**

| | |
|---|---|
| Dimensions | 400×200×10 ft |
| Number of grid cells | 30×15×1 |
| Porosity | 0.15 |
| ln mean permeability | 24.5 md |
| Dykstra-Parsons coefficient | 0.59 |
| Correlation length | x: 200 ft y: 100 ft z: 10 ft |
| Relative permeability model | Corey |
| Residual saturation ($W/L_1/G/L_2$*) | 0.4/0.2/0.05/0.05 |
| Endpoint relative permeability ($W/L_1/G/L_2$*) | 0.35/0.50/0.65/0.65 |
| Exponent ($W/L_1/G/L_2$*) | 3.0/3.0/3.0/3.0 |
| Initial saturation ($W/L_1/G/L_2$*) | 0.4/0.6/0.0/0.0 |

*$W$: aqueous phase; $L_1$: oleic phase; $G$: gaseous phase; $L_2$: $CO_2$-rich liquid phase.

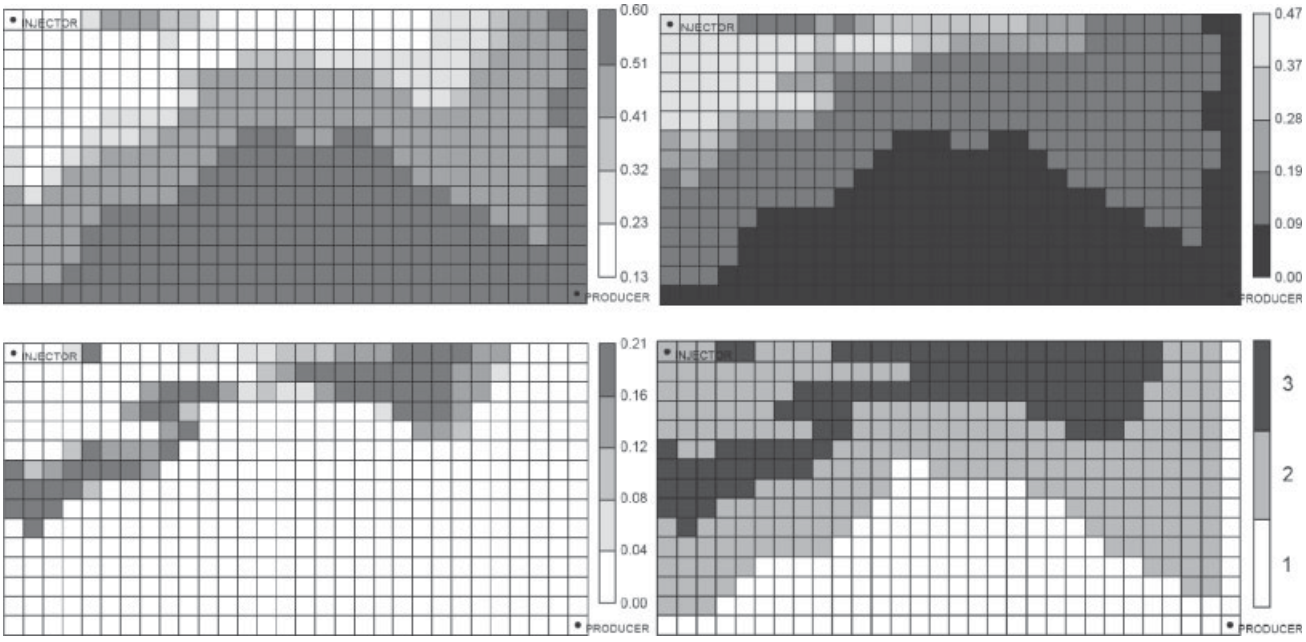


**Fig. 11—Top left: Saturation distribution of the oleic phase at 0.5 HCPVI for the NWE oil displacement. Top right: Saturation distribution of the gaseous phase at 0.5 HCPVI. Bottom left: Saturation distribution of the $CO_2$-rich liquid phase. Bottom right: Distribution of the number of hydrocarbon phases at 0.5 HCPVI.**

The injection well is operated at a constant injection rate of $10^4$ scf/D, while the production well produces at a constant bottomhole pressure of 930 psia.

**Fig. 11** shows saturation distributions and the distribution of the number of hydrocarbon phases at breakthrough, which is near 0.5 HCPVI. At this time, three hydrocarbon phases exist in 20% of the total grid cells, so that three-phase-equilibrium calculations play an important role in the simulation results. Simulations using (CSA, MG) and (RSA, RF) are almost identical with each other (Fig. 10). The computational time, however, depends significantly on the algorithm used. **Table 7** gives a breakdown of the computational times for the 10- and 20-component cases. The computational time with different $N_C$ is plotted in **Fig. 12** for each algorithm. Use of the reduced method results in simulations with shorter computational times than when (CSA, MG) is used for all cases studied here. The advantage of the reduced method against (CSA, MG) becomes more significant as $N_C$ increases. For example, the speed-up of the simulations is 12% for the 10-component case and 43% for the 20-component case. The speed-up is attributed to the decreased computational time in phase-equilibrium calculations with the second-order convergence methods, where the reduced method can exploit the decreased number of equations to be solved (Table 7). Fig. 12 shows that the Newton iteration with (RSA, RF) is 1.6 times and 3.6 times faster than with (CSA, MG) for the 10- and 20-component cases, respectively.

We also simulate this oil displacement using (CSA, MG) with the fluid characterization from Procedure A of Fong et al. (1992) described before (see Fig. 5). Three-phase-equilibrium calculations are not performed for this simulation. As expected, simulation results are significantly different from those with three-phase-equilibrium representations. Fig. 10 shows that breakthrough using fluid-characterization Procedure A occurs much earlier and that the oil recovery can be underpredicted by up to 5%. The deviation in recovery for this 2D reservoir simulation is much smaller than that for the 1D reservoir simulation shown in Fig. 6, indicating that the sweep efficiency is overpredicted using Procedure A.

Fig. 12 compares the computational times of simulations using (CSA, MG) with Procedure A, and (RSA, RF) and (CSA, MG) with the three-phase characterization. The computational time for the three-hydrocarbon-phase simulation with (RSA, RF) is 68% longer for 10 components and 31% longer for 20 components compared to the two-hydrocarbon-phase simulation with (CSA, MG). That is, the speed-up from using Procedure A becomes less significant as more components are used in the simulation. The three-hydrocarbon-phase simulation with (RSA, RF) using 10 components takes less computational time than the two-hydrocarbon-phase simulation with (CSA, MG) and Procedure A using 15 components. Similarly, (RSA, RF) using 15 components is faster than (CSA, MG) with Procedure A using 20 components. Fig. 12 also shows that the Newton iterations for phase-equilibrium calculations with (RSA, RF) in the three-hydrocarbon-phase simulation are faster than those with (CSA, MG) in the two-hydrocarbon-phase simulation for 10 or more components. This is a consequence of the reduced number of equations to be solved for (RSA, RF). For example, when more than 12 components are used, two-phase calculations with (CSA, MG) must solve more equations than three-phase calculations with (RSA, RF).

**TABLE 7—BREAKDOWN OF COMPUTATIONAL TIME F OR SIMULATIONS WITH THE NWE OIL**

| | | 10 components | | | | 20 components | | | |
|---|---|---|---|---|---|---|---|---|---|
| | | (RSA, RF) | | (CSA, MG) | | (RSA, RF) | | (CSA, MG) | |
| Overall simulation (seconds) | | 578.5 | 100% | 647.5 | 100% | 1,322.3 | 100% | 1,884.2 | 100% |
| Phase equilibrium calculations (seconds) | | 446.5 | 77% | 514.5 | 79% | 957.5 | 72% | 1,505.8 | 80% |
| Stability analysis (seconds) | SS | 289.3 | 50% | 291.5 | 45% | 663.7 | 50% | 689.1 | 37% |
| | Newton | 54.5 | 9% | 68.3 | 11% | 94.1 | 7% | 306.0 | 16% |
| Flash calculations (seconds) | SS | 43.5 | 8% | 44.0 | 7% | 94.5 | 7% | 97.3 | 5% |
| | Newton | 59.1 | 10% | 110.6 | 17% | 105.2 | 8% | 413.3 | 22% |

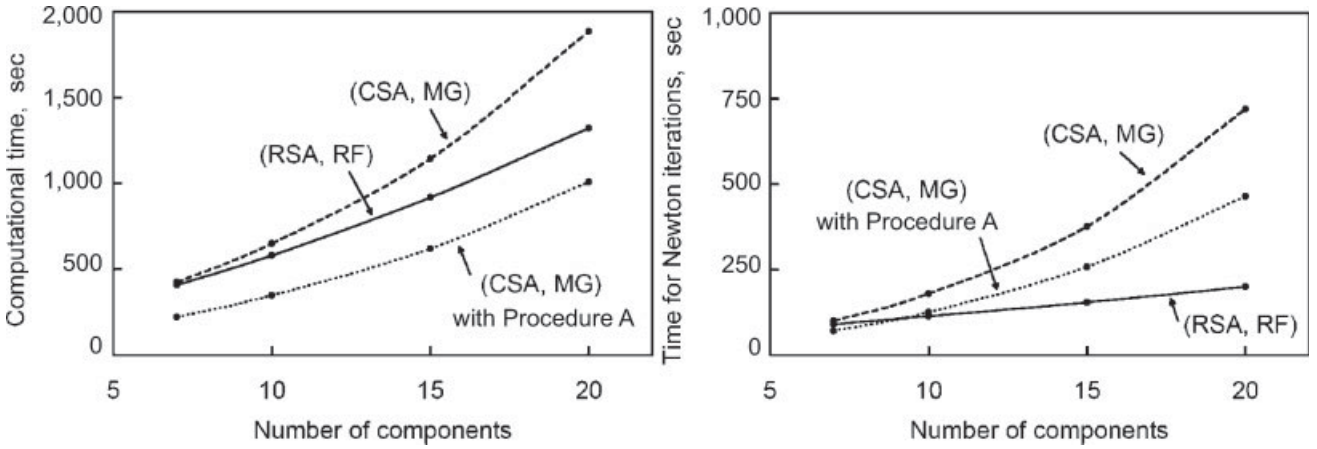


**Fig. 12—Left: Comparison of computational times with (RSA, RF), (CSA, MG), and (CSA, MG) with Procedure A for the NWE oil-displacement simulation. Right: Comparisons of computational times for phase-equilibrium calculations with the second-order convergence methods for the NWE oil displacement.**

**BSB Oil With a 2D Layered-Reservoir Model.** We next simulate an oil displacement with injection gas consisting of 5% $C_1$ and 95% $CO_2$ for 1.5 HCPVI in a 2D layered-reservoir model. The reservoir consists of three layers with different thicknesses, porosities, and permeabilities, as given in **Table 8.** The production and injection wells are open from the top to the bottom layer. The reservoir oil is the BSB oil (Khan et al. 1992), and the properties are shown in Table 4. The MMP with pure $CO_2$ was experimentally determined to be approximately 1,200 psia at reservoir temperature of 105°F (Khan et al. 1992). The injection well is operated at a constant bottomhole pressure of 1,300 psia, and the production well produces at a constant bottomhole pressure of 900 psia.

Three hydrocarbon phases form over a relatively small portion of the reservoir compared to the previous example with the NWE oil. **Fig. 13** shows phase saturations and the distribution of the number of phases at 0.4 HCPVI. At this time, three and two hydrocarbon phases exist in 11% and 36% of the total grid cells, respectively. Simulation results using (CSA, MG) and (RSA, RF) are nearly identical with each other **(Fig. 14). Table 9** shows a breakdown of the computational time for the 10- and 20-component cases. As in the previous NWE oil case, the use of (RSA, RF) can decrease the computational time significantly without loss of accuracy. **Fig. 15** compares the computational times with (RSA, RF) and (CSA, MG) for different $N_C$. For example, the speed-up from using (RSA, RF) is 17 and 39% for the 10- and 20-component cases, respectively. The speed-up mainly is attributed to the decreased computational time in the second-order convergence methods (Table 9). Fig. 15 compares the computational time spent in the Newton iteration for the stability and flash calculations. The Newton iteration with (RSA, RF) is 1.9 times and 4.2 times faster than that with (CSA, MG) for the 10- and 20-component cases, respectively.

Simulation with (RSA, RF) also exhibits significantly improved robustness compared to that with (CSA, MG). MG can fail to converge to a correct solution in the following three cases: (1) the line search cannot find lower Gibbs free energy, (2) independent phase component mole numbers are updated to be negative, and (3) convergence cannot be achieved within a specified number of iterations. The RF algorithm can fail to converge to a correct solution when it converges to a trivial solution and when it cannot converge within a specified number of iterations. The RF algorithm contains an iterative solution of the Rachford-Rice equations, but the minimization algorithm of Okuno et al. (2009b) guarantees convergence even for more than three phases.

**Fig. 16** shows the number of failures with varying $N_C$ for RF and MG. The failure rate of MG is much more sensitive to $N_C$ compared to that of RF. MG can suffer significantly from round-off errors in near-critical regions (Trangenstein 1987). The round-off errors become more severe when more components are used because the independent variables have smaller values. The RF algorithm also can suffer from round-off errors in near-critical regions, but the results show improved stability of the algorithm. To see the effect of $N_C$ on the condition number of the Hessian matrix for MG, we consider the mixture of the BSB oil and gas that is at the same conditions as in the example calculation in the Standalone Three-Phase Flash Calculations section. The condition number of the Hessian matrix for MG is $1.3\times10^{10}$ for seven components and $1.8\times10^{11}$ for 20 components. The increase in the condition number by one order of magnitude can affect the failure rate of MG significantly because millions of flash calculations

**TABLE 8—RESERVOIR PROPERTIES FOR THE SIMULATION CASE STUDY WITH THE BSB OIL**

| | |
|---|---|
| Dimensions | 500×10×45 ft |
| Number of grid cells | 50×1×9 |
| Thickness (top/middle/bottom) (ft) | 20.0/10.0/15.0 |
| Porosity (top/middle/bottom) | 0.08/0.10/0.09 |
| Permeability (top/middle/bottom) (md) | 7.0/11.2/9.8 |
| Relative permeability model | Corey |
| Residual saturation ($W/L_1/G/L_2$*) | 0.4/0.2/0.05/0.05 |
| Endpoint relative permeability ($W/L_1/G/L_2$*) | 0.35/0.50/0.65/0.65 |
| Exponent ($W/L_1/G/L_2$*) | 3.0/3.0/3.0/3.0 |
| Initial saturation ($W/L_1/G/L_2$*) | 0.4/0.6/0.0/0.0 |

*$W$: aqueous phase; $L_1$: oleic phase; $G$: gaseous phase; $L_2$: $CO_2$-rich liquid phase.

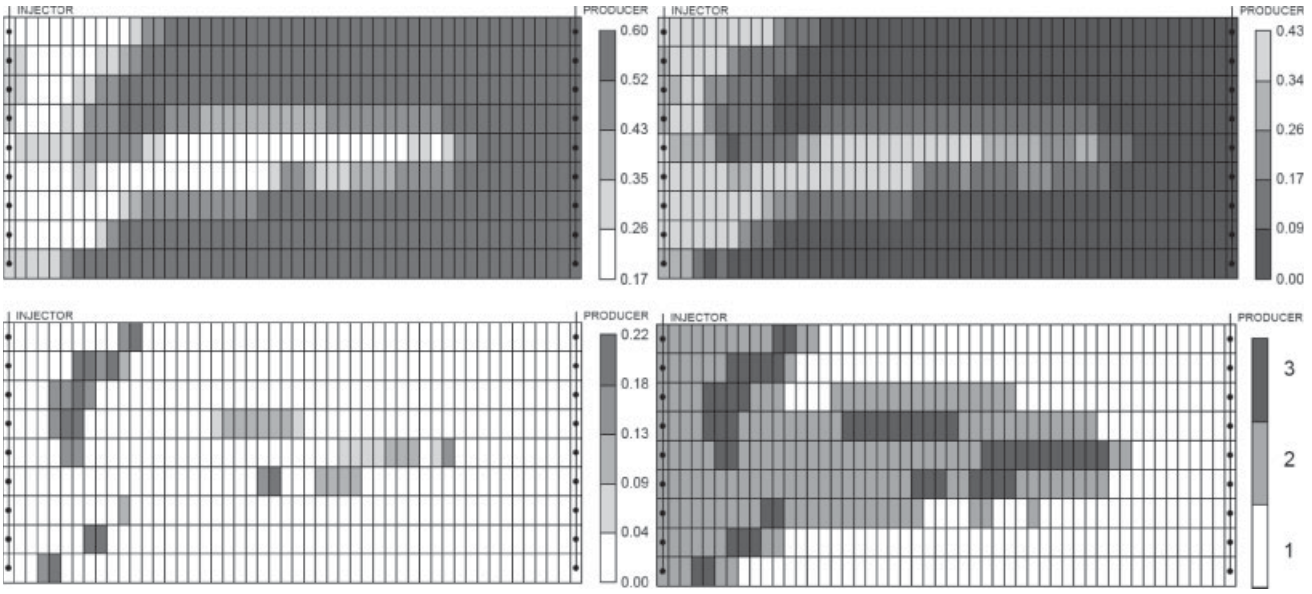


**Fig. 13—Top left: Saturation distribution of the oleic phase at 0.4 HCPVI for the BSB oil displacement. Top right: Saturation distribution of the gaseous phase at 0.4 HCPVI. Bottom left: Saturation distribution of the $CO_2$-rich liquid phase at 0.4 HCPVI. Bottom right: Distribution of the number of hydrocarbon phases at 0.4 HCPVI.**

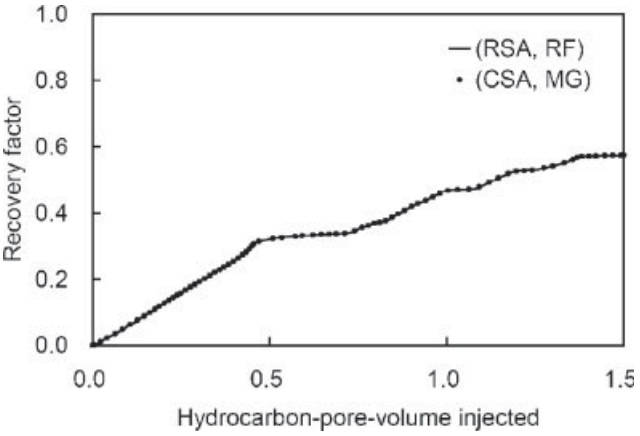


**Fig. 14—Recovery factors for the BSB oil-displacement simulations using (RSA, RF) and (CSA, MG) are nearly identical to each other.**

typically are performed in near-critical regions for simulation of multicontact miscible gasfloods.

The increased failure rate of MG decreases the timestep size for the simulation using UTCOMP because of discontinuous changes in physical parameters, such as phase saturation and density. The decreased timestep size, in turn, increases the frequency of the solution of the pressure equations for the IMPEC scheme. For that reason, the 20-component case solves the pressure equations 163 more times than the seven-component case. Fig. 16 shows that the number of pressure-equation solutions required increases as the failures in three-phase flash calculations increase. Failures in flash calculations can decrease the timestep sizes substantially, as shown in **Fig. 17,** where, for illustration, timesteps are shown over a small portion of the total simulation time. Fig. 17 also shows that the timestep size is more stable for simulations with (RSA, RF) than for simulations with (CSA, MG) because of the four failures of MG. Those results demonstrate that robustness of phase-equilibrium algorithms can affect the efficiency of the simulation not only through phase-equilibrium calculations themselves but also through a reduction of the timestep sizes. Also, if stability analysis fails to predict correctly that three hydrocarbon phases exist, the resulting false two-phase solution could cause a reduction in the timestep sizes (see the Use of Two-Phase Flash in a Three-Phase Region subsection). The speed-up as the result of improved timestep sizes would be more significant when more grid cells are used because the system of pressure equations becomes larger and pressure-equation solutions are costly.

When a flash calculation fails to converge to the correct solution, UTCOMP, in general, does not repeat the same calculation using a different algorithm. UTCOMP continues the simulation, but a timestep size is decreased to alleviate a large change in physical properties over the timestep. There is another possible way to handle this. When the primary flash algorithm fails to converge to the correct solution, a simulator can attempt to solve the same flash problem using a more robust, but typically very time-consuming, algorithm. For such a simulator, flash failures also directly increase the total computational time of the simulation.

**TABLE 9—BREAKDOWN OF COMPUTATIONAL TIME F OR SIMULATIONS WITH THE BSB OIL**

| | | 10 components | | | | 20 components | | | |
|---|---|---|---|---|---|---|---|---|---|
| | | (RSA, RF) | | (CSA, MG) | | (RSA, RF) | | (CSA, MG) | |
| Overall simulation (seconds) | | 1,225.4 | 100% | 1,434.4 | 100% | 2,849.9 | 100% | 3,967.5 | 100% |
| Phase equilibrium calculations (seconds) | | 973.9 | 79% | 1,175.5 | 82% | 2,133.7 | 75% | 3,224.9 | 81% |
| Stability analysis (seconds) | SS | 553.2 | 45% | 581.7 | 41% | 1,282.1 | 45% | 1,341.4 | 34% |
| | Newton | 53.5 | 4% | 86.1 | 6% | 88.1 | 3% | 378.3 | 10% |
| Flash calculations (seconds) | SS | 235.6 | 19% | 240.8 | 17% | 529.3 | 19% | 545.3 | 14% |
| | Newton | 131.7 | 11% | 266.9 | 19% | 234.1 | 8% | 959.9 | 24% |

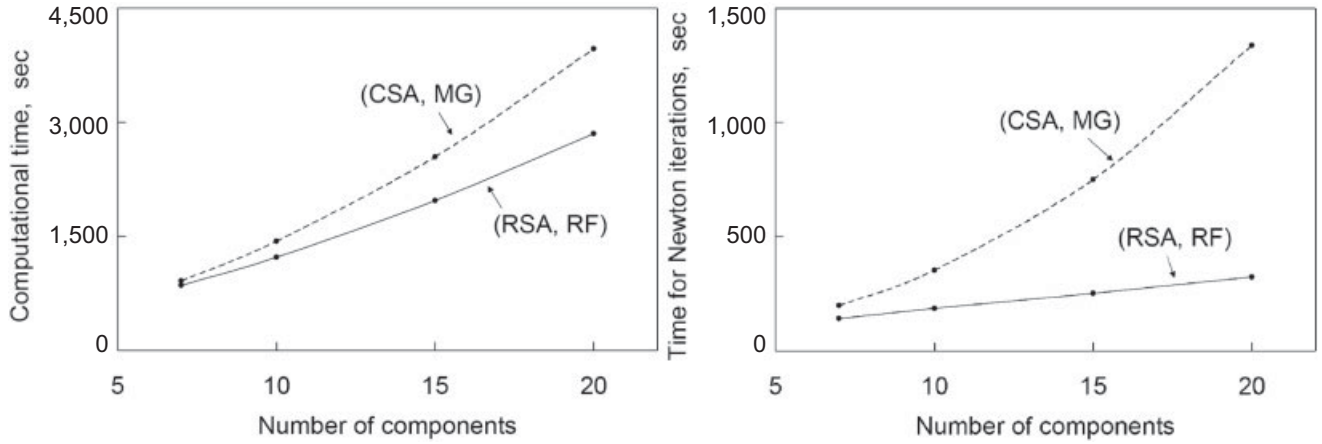


**Fig. 15—Left: Comparison of computational times with (RSA, RF) and (CSA, MG) for the BSB oil-displacement simulation. Right: Comparisons of computational times for phase-equilibrium calculations with the second-order convergence methods for the BSB oil displacement.**

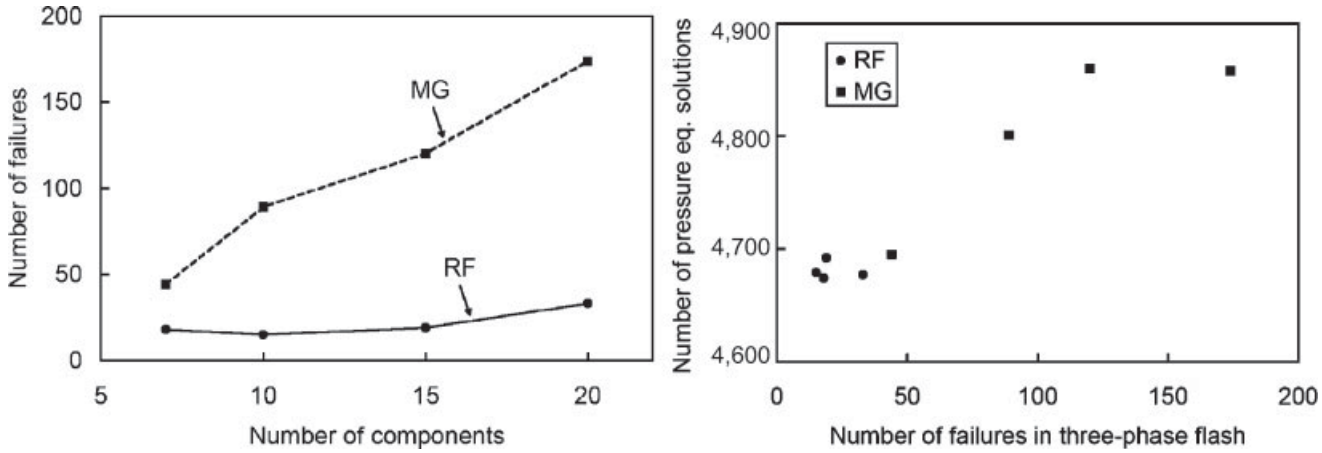


**Fig. 16—Left: Comparison of the number of failures in three-phase flash calculations with the RF algorithm and MG for different numbers of components for the BSB oil displacement. Right: Frequency of solution of pressure equations during the simulation is positively correlated with the number of failures in three-phase flash calculations.**

## Conclusions

We investigated the importance of three-phase-equilibrium calculations in simulation of low-temperature gasfloods. We developed an efficient and robust algorithm for three-phase flash calculations using a reduced method. The algorithm was implemented in a multiphase compositional simulator, UTCOMP, to demonstrate the efficiency and robustness in simulations using different fluids, numbers of components, and reservoir models. The results show that

- The two-phase-equilibrium approximations proposed in the literature can lead to a complete failure of simulation or to erroneous simulation results.
- Use of the reduced method can decrease the computational time significantly without loss of accuracy. For the cases studied, simulations with the three-phase reduced method using 10 components take less computational time than simulations with conventional methods using 15 components assuming only two phases exist.
- Compared to the standard algorithms used in this research, the reduced method exhibits improved efficiency and robustness, especially when more components are used in the simulation.
- On the basis of the simulation case studies using UTCOMP, the robust three-phase flash with the reduced method decreases the computational time not only because of the flash calculations themselves but also because of improved timestep sizes.
- Because of the significant speed-up, use of the reduced method can allow for more components to be used in the simulation. Using more components in reservoir simulation can improve accuracy of the fluid characterization and reservoir/surface integrated modeling.

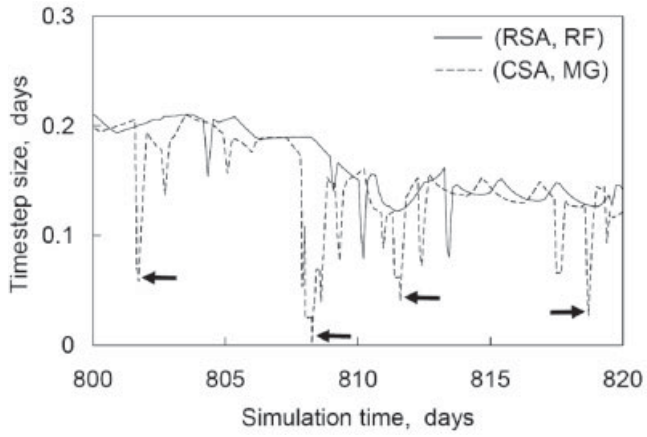


**Fig. 17—Variation of timestep sizes for simulations with (RSA, RF) and (CSA, MG). The four arrows indicate failure points of MG for three-phase flash calculations. There are no failures for the RF algorithm within this time window.**

## Nomenclature

$A_i$ = EOS parameter for component $i$
$B_i$ = EOS parameter for component $i$
$F_{ij}$ = fugacity equation for component $i$ in phase $j$
$F_j^R$ = $j$th equation for reduced flash calculations
$g_i$ = parameter of component $i$ for the reduced method
$h_i$ = parameter of component $i$ for the reduced method
$k_{ij}$ = binary interaction coefficient between components $i$ and $j$
$K_{ij}$ = $K$-value for component $i$ in phase $j$
$L_1$ = oleic phase
$L_2$ = solvent-rich liquid phase
$N_C$ = number of components
$P_C$ = critical pressure
$S_i$ = stationarity equation for component $i$
$S_j$ = saturation of phase $j$
$T_C$ = critical temperature
$V$ = gaseous phase
$x_{ij}$ = mole fraction of component $i$ in phase $j$
$z_i$ = mole fraction of component $i$ in a mixture
$Z_j$ = compressibility factor for phase $j$
$\beta_j$ = mole fraction of phase $j$
$\varepsilon$ = stopping criteria for iterative solution
$\eta_{ki}$ = constant term for component $i$ to define $k$th reduced parameter
$\theta_{kj}$ = $k$th reduced parameter in phase $j$
$\underline{\theta}_j$ = vector with elements $\theta_{kj}$ for $k = 1,\ldots,5$
$\varphi_{ij}$ = fugacity coefficient for component $i$ in phase $j$

## Acknowledgments

We thank the Japan Petroleum Exploration Company and the Japan Oil, Gas and Metals National Corporation for support of this research, along with the member companies of the Gas Flooding Joint-Industry Project at The University of Texas at Austin.

## References

Alwani, Z. and Schneider, G.M. 1976. Fluid Mixtures at High Pressure. Phase Separation and Critical Phenomena in Binary Mixtures of a Polar Component With Supercritical Carbon Dioxide, Ethane, and Ethene up to 1000 Bar. *Berichte der Bunsengesellschaft fuer Physikalische Chemie* **80** (12): 1310–1315.

Chang, Y.-B. 1990. *Development and Application of an Equation of State Compositional Simulator*. PhD dissertation, University of Texas at Austin, Austin, Texas.

Chang, Y.-B., Pope, G.A., and Sepehrnoori, K. 1990. A Higher-Order Finite-Difference Compositional Simulator. *J. Pet. Sci. Eng.* **5** (1): 35–50. doi: 10.1016/0920-4105(90)90004-M.

Creek, J.L. and Sheffield, J.M. 1993. Phase Behavior, Fluid Properties, and Displacement Characteristics of Permian Basin Reservoir Fluid/$CO_2$ Systems. *SPE Res Eng* **8** (1): 34–42. SPE-20188-PA. doi: 10.2118/20188-PA.

Evelein, K.A., Moore, R.G., and Heidemann, R.A. 1976. Correlation of the Phase Behavior in the Systems Hydrogen Sulfide-Water and Carbon Dioxide-Water. *Ind. Eng. Chem. Process Des. Dev.* **15** (3): 423–428. doi: 10.1021/i260059a013.

Firoozabadi, A. and Pan, H. 2002. Fast and Robust Algorithm for the Compositional Modeling: Part I. Stability Analysis Testing. *SPE J.* **7** (1):78–89. SPE-77299-PA. doi: 10.2118/77299-PA.

Fong, W.S., Sheffield, R.E., and Emanuel, A.S. 1992. Phase Modeling Techniques for Low-Temperature $CO_2$ Applied to McElroy and North Ward Estes Projects. Paper SPE 24184 presented at the SPE/DOE Enhanced Oil Recovery Symposium, Tulsa, 22–24 April. doi: 10.2118/24184-MS.

Gill, P.E. and Murray, W. 1974. Newton-Type Methods for Unconstrained and Linearly Constrained Optimization. *Mathematical Programming* **7** (3): 311–350. doi: 10.1007/BF01585529.

Guler, B., Wang, P., Delshad, M., Pope, G.A., and Sepehrnoori, K. 2001. Three- and Four-Phase Flow Compositional Simulations of $CO_2$/NGL EOR. Paper SPE 71485 presented at the SPE Annual Technical Conference and Exhibition, New Orleans, 30 September–3 October. doi: 10.2118/71485-MS.

Hendriks, E.M. 1988. Reduction Theorem for Phase Equilibrium Problems. *Ind. Eng. Chem. Res.* **27** (9): 1728–1732. doi: 10.1021/ie00081a027.

Hendriks, E.M. and van Bergen, A.R.D. 1992. Application of a Reduction Method to Phase Equilibria Calculations. *Fluid Phase Equilibria* **74:** 17–34. doi: 10.1016/0378-3812(92)85050-I.

Henry, R.L. and Metcalfe, R.S. 1983. Multiple-Phase Generation During Carbon Dioxide Flooding. *SPE J.* **23** (4): 595–601. SPE-8812-PA. doi: 10.2118/8812-PA.

Hoteit, H. and Firoozabadi, A. 2006. Simple Phase Stability-Testing Algorithm in the Reduction Method. *AIChE Journal* **52** (8): 2909–2920. doi: 10.1002/aic.10908.

Jensen, B.H. and Fredenslund, A. 1987. A Simplified Flash Procedure for Multicomponent Mixtures Containing Hydrocarbons and one Non-Hydrocarbon Using Two-Parameter Cubic Equations of State. *Ind. Eng. Chem. Res.* **26** (10): 2129–2134. doi: 10.1021/ie00070a032.

Kaul, P. and Thrasher, R.L. 1996. A Parameter-Based Approach for Two-Phase-Equilibrium Prediction With Cubic Equations of State. *SPE Res Eng* **11** (4): 273–279. SPE-26640-PA. doi: 10.2118/26640-PA.

Khan, S.A. 1992. *An Expert System to Aid in Compositional Simulation of Miscible Gas Flooding*. PhD dissertation, University of Texas at Austin, Austin, Texas (December 1992).

Khan, S.A., Pope, G.A., and Sepehrnoori, K. 1992. Fluid Characterization of Three-Phase $CO_2$/Oil Mixtures. Paper SPE 24130 presented at the SPE/DOE Enhanced Oil Recovery Symposium, Tulsa, 22–24 April. doi: 10.2118/24130-MS.

Leibovici, C.F., Barker, J.W., and Waché, D. 2000. Method for Delumping the Results of Compositional Reservoir Simulation. *SPE J.* **5** (2): 227–235. SPE-64001-PA. doi: 10.2118/64001-PA.

Li, Y. and Johns, R.T. 2006. Rapid Flash Calculations for Compositional Simulation. *SPE Res Eval & Eng* **9** (5): 521–529. SPE-95732-PA. doi: 10.2118/95732-PA.

Liu, J., Delshad, M., Pope, G.A., and Sepehrnoori, K. 1994. Application of Higher-Order Flux-Limited Methods in Compositional Simulation. *Transport in Porous Media* **16** (1): 1–29. doi: 10.1007/BF01059774.

Michelsen, M.L. 1982a. The Isothermal Flash Problem. Part I. Stability. *Fluid Phase Equilibria* **9** (1): 1–19. doi: 10.1016/0378-3812(82)85001-2.

Michelsen, M.L. 1982b. The Isothermal Flash Problem. Part II. Phase-Split Calculation. *Fluid Phase Equilibria* **9** (1): 21–40. doi: 10.1016/0378-3812(82)85002-4.

Michelsen, M.L. 1986. Simplified Flash Calculations for Cubic Equations of State. *Ind. Eng. Chem. Process Des. Dev.* **25** (1): 184–188. doi: 10.1021/i200032a029.

Miller, M.M. and Luks, K.D. 1989. Observations on the Multiphase Equilibria Behavior of $CO_2$-Rich and Ethane-Rich Mixtures. *Fluid Phase Equilibria* **44** (3): 295–304. doi: 10.1016/0378-3812(89)80059-7.

Nghiem, L.X. and Li, Y.-K. 1984. Computation of Multiphase Equilibrium Phenomena with an Equation of State. *Fluid Phase Equilibria* **17** (1): 77–95. doi: 10.1016/0378-3812(84)80013-8.

Nghiem, L.X. and Li, Y.K. 1986. Effect of Phase Behavior on $CO_2$ Displacement Efficiency at Low Temperatures: Model Studies With an Equation of State. *SPE Res Eng* **1** (4): 414–422. SPE-13116-PA. doi: 10.2118/13116-PA.

Nichita, D.V., Broseta, D., and de Hemptinne, J.-C. 2006. Multiphase Equilibrium Calculation Using Reduced Variables. *Fluid Phase Equilibria* **246** (1–2): 15–27. doi: 10.1016/j.fluid.2006.05.016.

Nichita, D.V., Gomez, S., and Luna, E. 2002. Phase Stability Analysis With Cubic Equations of State by Using a Global Optimization Method. *Fluid Phase Equilibria* **194–197:** 411–437. doi: 10.1016/S0378-3812(01)00779-8.

Okuno, R. 2009. *Modeling of Multiphase Behavior for Gas Flooding Simulation*. PhD dissertation, University of Texas at Austin, Austin, Texas (August 2009).

Okuno, R., Johns, R.T., and Sepehrnoori, K. 2009a. Application of a Reduced Method in Compositional Simulation. Accepted for *SPE J.* SPE-119657-PA. doi: 10.2118/119657-PA.

Okuno, R., Johns, R.T., and Sepehrnoori, K. 2009b. A New Algorithm for Rachford-Rice for Multiphase Compositional Simulation. Accepted for *SPE J.* SPE-117752-PA. doi: 10.2118/117752-PA.

Orr, F.M. Jr., Yu, A.D., and Lien, C.L. 1981. Phase Behavior of $CO_2$ and Crude Oil in Low-Temperature Reservoirs. *SPE J.* **21** (4): 480–492. SPE-8813-PA. doi: 10.2118/8813-PA.

Pan, H. and Firoozabadi, A. 2003. Fast and Robust Algorithm for Compositional Modeling: Part II—Two-Phase Flash Computations. *SPE J.* **8** (4): 380–391. SPE-87335-PA. doi: 10.2118/87335-PA.

Peng, D-Y. and Robinson, D.B. 1976. A New Two-Constant Equation of State. *Ind. Eng. Chem. Fund.* **15** (1): 59–64. doi: 10.1021/i160057a011.

Perschke, D.R. 1988. *Equation of State Phase Behavior Modeling for Compositional Simulation*. PhD dissertation, University of Texas at Austin, Austin, Texas.

Perschke, D.R., Chang, Y.-B., Pope, G.A., and Sepehrnoori, K. 1989. Comparison of Phase Behavior Algorithms for an Equation-of-State Compositional Simulator. Paper SPE 19443 available from SPE, Richardson, Texas.

Rachford, H.H. Jr. and Rice, J.D. 1952. Procedure for Use of Electronic Digital Computers in Calculating Flash Vaporization Hydrocarbon Equilibrium (Technical Note 136). *J Pet Technol* **4** (10): 19; *Trans.,* AIME, **195:** 327–328. SPE-952327-G.

Shelton, J.L. and Yarborough, L. 1977. Multiple Phase Behavior in Porous Media During $CO_2$ or Rich-Gas Flooding. *J Pet Technol* **29** (9): 1171–1178. SPE-5827-PA. doi: 10.2118/5827-PA.

Trangenstein, J.A. 1987. Customized Minimization Techniques for Phase Equilibrium Computations in Reservoir Simulation. *Chemical Engineering Science* **42** (12): 2847–2863. doi: 10.1016/0009-2509(87)87051-3.

Turek, E.A., Metcalfe, R.S., and Fishback, Robert E. 1988. Phase Behavior of Several $CO_2$/West-Texas-Reservoir-Oil Systems. *SPE Res Eng* **3** (2): 505–516. SPE-13117-PA. doi: 10.2118/13117-PA.

van Konynenburg, P.H. and Scott, R.L. 1980. Critical Lines and Phase Equilibria in Binary van der Waals Mixtures. *Phil. Trans. R. Soc. Lond. A* **298** (1442): 495–540. doi: 10.1098/rsta.1980.0266.

Wang, X. and Strycker, A. 2000. Evaluation of $CO_2$ Injection with Three Hydrocarbon Phases. Paper SPE 64723 presented at the International Oil and Gas Conference and Exhibition in China, Beijing, 7–10 November. doi: 10.2118/64723-MS.

Wilson, G.M. 1969. A Modified Redlich-Kwong Equation of State, Application to General Physical Data Calculations. Paper 15-C presented at the 65th National AIChE Meeting, Cleveland, Ohio, USA, 4–7 May.

## Appendix A

**Fig. A-1** is a flow chart of multiphase equilibrium calculations in UTCOMP from Chang (1990).

## Conversion Factors

| | | |
|---|---|---|
| ft | × 3.048* | E–01 = m |
| °F | (°F–32)/1.8 | = °C |
| psi | × 6.894 757 | E+00 = kPa |

*Conversion factor is exact.

**Ryosuke Okuno** is a reservoir engineer with the Japan Petroleum Exploration Company in Tokyo. His research interests include phase-behavior modeling and compositional reservoir simulation. Okuno holds BS and MS degrees in geosystem engineering from the University of Tokyo and a PhD degree in petroleum engineering from the University of Texas at Austin. **Russell T. Johns** is the B.L. Lancaster Professor in the Department of Petroleum and Geosystems Engineering at the University of Texas at Austin. His research interests include theory of gas-injection processes, multiphase flow in porous media, and well testing. Johns holds a BS degree in electrical engineering from Northwestern University and MS and PhD degrees in petroleum engineering from Stanford University. **Kamy Sepehrnoori** is the Bank of America Professor in the Department of Petroleum and Geosystems Engineering at the University of Texas at Austin. His research and teaching interests include computational methods, reservoir simulation, parallel computations, enhanced-oil-recovery modeling, and inverse modeling. He holds a PhD degree from the University of Texas at Austin.

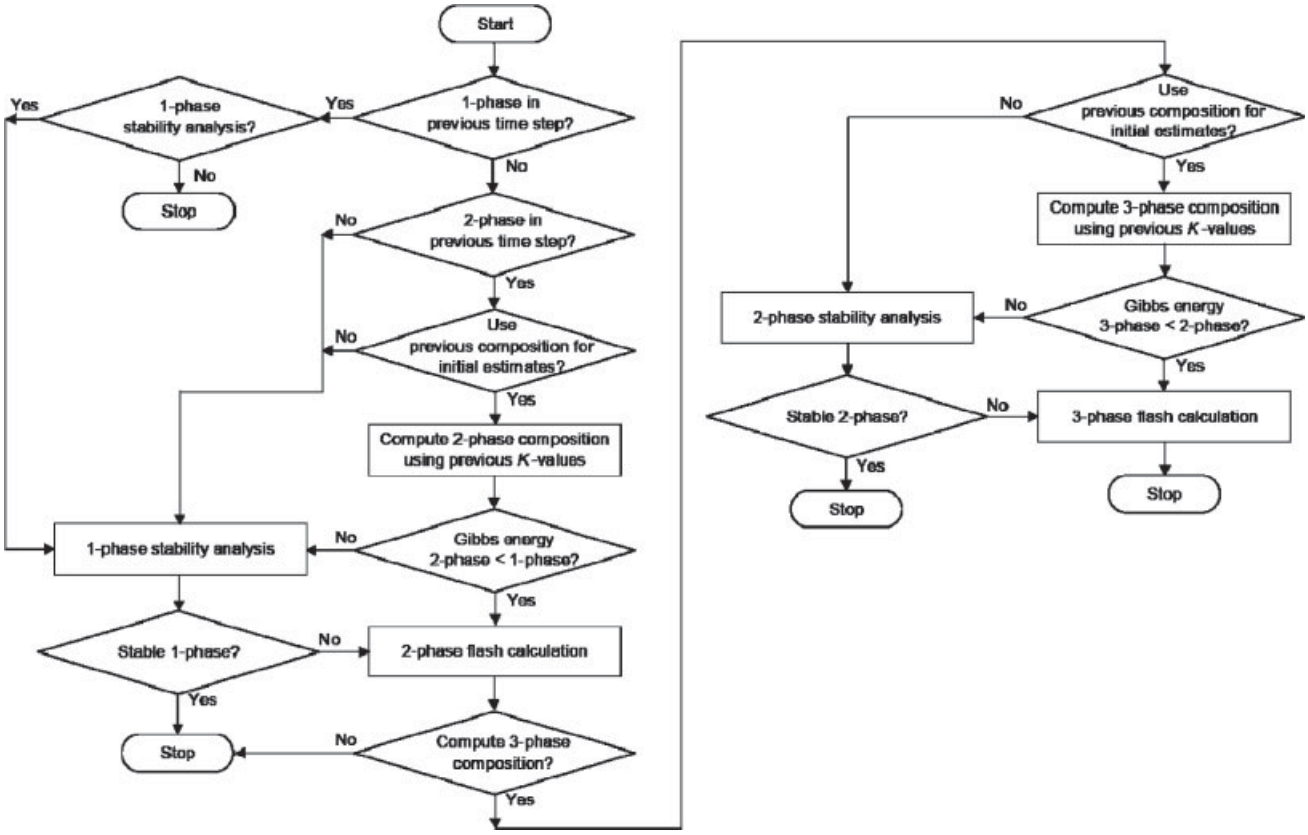


**Fig. A-1—A flow chart of multiphase equilibrium calculations in UTCOMP.**